PONTIFICIA UNIVERSIDAD CATOLICA DE CHILE
ESCUELA DE INGENIERÍA

SPECTRAL ELEMENTS FOR MULTIPLE TRACE FORMULATION APPLIED TO SCATTERING PROBLEMS IN TWO DIMENSION.

JOSÉ ANDRÉS PINTO DENEGRI

Thesis submitted to the Office of Research and Graduate Studies
in partial fulfillment of the requirements for the degree of
Master of Science in Engineering

Advisor:
CARLOS JEREZ-HANCKES

Santiago de Chile, June 2015

PONTIFICIA UNIVERSIDAD CATOLICA DE CHILE
ESCUELA DE INGENIERÍA

SPECTRAL ELEMENTS FOR MULTIPLE TRACE FORMULATION APPLIED TO SCATTERING PROBLEMS IN TWO DIMENSION.

JOSÉ ANDRÉS PINTO DENEGRI

Members of the Committee:
CARLOS JEREZ-HANCKES
MIGUEL RÍOS
MATIAS COURDURIER
ESTEBAN SAEZ

Thesis submitted to the Office of Research and Graduate Studies
in partial fulfillment of the requirements for the degree of
Master of Science in Engineering

Santiago de Chile, June 2015

To my family.

ACKNOWLEDGEMENTS

First, I thank God and my family for all their support and love, without them this work would have been impossible.

I want to thank Professor Carlos Jerez, who has been an excellent advisor as well as a person and has always motivated me to continue with my research. Special thanks to Simon Tournier for his help during the development of this work. I can not omit the other members of the research team, Juan Bozzo, Fernando Henríquez, and Gerardo Silva with whom I have worked on multiples projects during these last two years.

I would also like to thank all the members of the Futsal team of Pontificia Universidad Católica and the coach Ricardo Rodríguez. Though they are not direct contributors to this thesis, they made my stay at the university very special and enjoyable.

Finally, i would want to thanks someone who i never meet on person, but was one of the most influential persons in construct who i am, Eduardo Bonvallet, rest in peace ”Guru”.

TABLE OF CONTENTS

LIST OF FIGURES

LIST OF TABLES

ABSTRACT

We present an efficient method to solve high-frequency scattering problems by heterogenous penetrable objects in two dimensions. This is achieved by extending the so-called *Local Multiple Traces Formulation*, introduced recently by Hiptmair & Jerez-Hanckes, to purely spectral discretizations employing weighted Chebyshev polynomials. Together with regularization strategies to handle boundary integral operators singularities, matrix entries are quickly computed via the Fast Fourier Transform. The resulting Fredholm first-kind formulation is free from spurious resonances, and though ill-conditioned, it possesses built-in preconditioners based on Calderón-type techniques. Numerical results are presented in order to validete obtained for different settings validate the previous claims and greatly motivate future research in this direction.

Keywords: **Boundary integral equations; spectral elements; multiple traces formulation; preconditioning; high-frequency scattering**.

RESUMEN

Un método eficiente para resolver problemas de difracción en alta frecuencia para dominios heterogéneos es presentado. Esto se logra extendiendo la *Formulación de Múltiples Trazas Locales*, introducida recientemente por Hiptmair & Jerez-Hanckes, a una discretización puramente espectral que emplea polinomios de Chebyshev con pesos. Esto junto con estrategias para manejar las singularidades de los operadores integrales, permite emplear la transformada rápida de Fourier para calcular las entradas de la matriz. El resultado es una formulación de Fredholm de primer tipo, libre de resonancias espurias, que aunque mal condicionada, tiene un precondicionador natural basado en la identidad de Calderón. Resultados numéricos para diferentes configuraciones son presentados con el objetivo de validar los puntos anteriores, y además motivan a seguir investigando en esta línea.

Keywords: **Ecuaciones integrales de frontera; elementos espectrales; formulación de múltiples trazas; precondicionamiento; difracción en alta frecuencia**.

1. INTRODUCTION

1.1. Basic Notation

$\mathbb{R}^d$: The d-dimensional real space with Euclidean norm, and usual topology,

$L^2(\Omega)$: The space of class of the square integrable functions on the domain Ω ,

$\mathbf{x}$: Bold variables represent vectors in $\mathbb{R}^d$,

$\mathbf{0}$: Zero vector in $\mathbb{R}^d$,

$\|\mathbf{x}\|$: Euclidean norm of $\mathbf{x} \in \mathbb{R}^d$,

$\|\mathbf{x}\|_\infty$: $\max_{i=1\ldots d} |x_i|$,

$(a, b)_V$: Interior product on V between vectors a and b,.

$\lfloor s \rfloor$: Lower integer part of a real number s, ie. $\lfloor 0.28 \rfloor = 0$,

$\bar{A}$: Closure of a set $A \subset \mathbb{R}^d$,

$B(x_0, r)$: Open ball centered on x_0 and radius r on $\mathbb{R}^d$,

$\mathcal{C}^k(\Omega)$: Space of k-times continuously differentiable functions on Ω,

$\mathcal{C}_0^k(\Omega)$: Subset of $\mathcal{C}^k(\Omega)$ of functions with compact support on Ω ,

$(V)'$: Topological dual of a vectorial space V,

$H_k^{(1)}$: Hankel function of first kind and order k see (Abramowitz, 1988),

$\mathrm{span}\{\mathbf{x}_1, \ldots, \mathbf{x}_n\}$: Vectorial space generated by vectos $\mathbf{x}_1 \ldots, \mathbf{x}_n$.

1.2. Scattering Problems

The scattering problems are the ones related to the collision of waves with solid materials. In particular there are two main problems, the direct scattering problem where a known incident wave illuminate a known solid domain so the scattered wave has to be found, and the inverse scattering problem, were the incident and scattering wave are known and one search for the form and proprieties of the domain.

The theory of scattering problems has been an important field of studies during the last century with numbers of works and applications. Is important to mention that the theory was rapidly pushed for the need of its applications, especially the radar and it usage for the armies. Now at days its applications include design of antennas (Sadiku, 1992),the analysis of defects on semiconductors (Niu, Luo, & Liu, 2014), radar imaging (Borden, 1999) and biomedical imaging (Ammari, 2008). In the following, we will proceed with a more depth description of the direct scattering problem that will be the motivation of the studies of this thesis.

Consider a bounded penetrable object Ω in the two dimensional space. This object is illuminated by an incident wave, and as a result, part of the wave penetrates the object and part is scattered to the exterior medium, where it recombines with the incident wave. The direct scattering problem is to find the scattered wave[1], where the properties of the domain Ω and the incident wave are known. The situation is illustrated on figure 1.1

The problem can be physically interpreted as an acoustic or electromagnetic one, depending of the nature of the incident wave. On both cases, we write the time dependence

[1]Defined in the whole space as the one that penetrates inside Ω and the ones that is scattered to the exterior medium outside of Ω

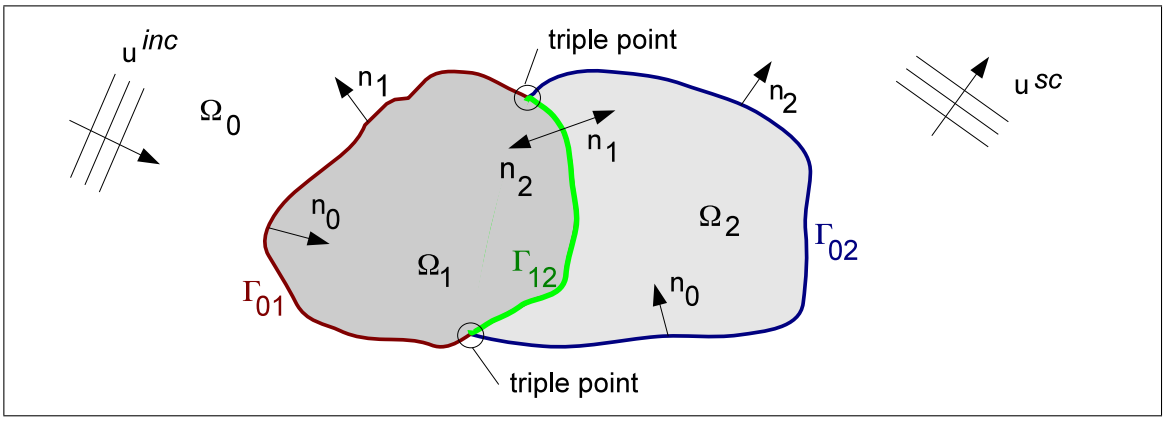

Figure 1.1. Direct scattering problem in Ω which is composed of two domains $\Omega = \Omega_1 \cup \Omega_2$

of the wave as:

$$U(x, y, t) = u(x, y)e^{i\omega t}, \tag{1.1}$$

where ω is the angular frequency. Then the wave equation (or Maxwell equations in case of electromagnetic) can be reduced to the Helmholtz equation see (Jin, 2011) (Section 4.2). This means that the equation for the scattered wave is the following:

$$(\Delta + \kappa^2)u = 0, \tag{1.2}$$

where $u(x, y)$ denotes the amplitude of the scattered wave at a point (x, y). In general, the quantity u is complex-valued and has to be interpreted as a phasor (Jin, 2011) (Section 1.7). Notice that the problem consists in finding u over the whole two dimensional space, so it is not a bounded problem.

The quantity κ in equation (1.2) is called wave number. In the Electromagnetic case can be defined as:

$$\kappa = \sqrt{\epsilon\mu}\omega, \tag{1.3}$$

where ϵ, μ are the electrical parameters [2] of Ω. The wave number is not constant on the space, but it will be assumed that it is constant outside of Ω and piecewise constant inside [3] . Moreover, if κ_0 denotes the exterior wave number and $(\kappa_i)_{i\geq 1}$ the finite values in the interior, then it will be assumed the following for the wave numbers:

$$\kappa_0 = \omega, \tag{1.4}$$

$$\kappa_i = \sqrt{\epsilon_i}\kappa_0. \tag{1.5}$$

Aside of the Helmholtz equation, the scattered wave fulfills the Sommerfeld radiation condition (Sommerfeld, 1949). This condition forces the scattered wave to irradiate towards infinity, instead of coming from infinity to Ω. Mathematically, it is expressed as follows:

$$\lim_{\|\mathbf{x}\|\to\infty} \|\mathbf{x}\|^{\frac{1}{2}} \left(\frac{\partial}{\partial\|\mathbf{x}\|} - ik\right) u(\mathbf{x}) \quad = \quad 0. \tag{1.6}$$

1.3. Mathematical Tools

As previously mentioned, a mathematical background is required to correctly formulate the scattering problem. Later, it will be clear that these tools are not only useful to state the problem, but also necessary for the study of the numerical scheme that will be implemented on this thesis. In this Section, we define some basic concepts and present classical results. None of the results are new so proofs are omitted, and they can be found on the monographs by (Sauter & Christoph, 2010) or (Steinbach, 2008) and references therein. Also refer to Section 1.1 for basic notation.

Let Ω denote an arbitrary open and bounded subset of $\mathbb{R}^d$, and let Γ denote the boundary $\partial\Omega$ that will be assumed to be compact. The open complement of Ω will be denoted

[2] Permittivity and Permeability.

[3] Ω could be divided in finite disjoint subsets with positive area, where the wave number is constant

$\Omega_0 := \mathbb{R}^d \backslash \overline{\Omega}$. Notions of smoothness of the physical domains are introduced in the following.

Definition 1.1. *The domain Ω is called Lipschitz if there is a finite open cover $\{G_i\}_{i\in I}$ and a family of mappings $\{F_i : \overline{B(0,1)} \mapsto \overline{G_i}\}_{i\in I}$ such that*

(i) *F_i is bijective* $\quad \forall i \in I$,

(ii) *F_i, F_i^{-1} are Lipschitz maps,and*

(iii) *the image of the upper half of $\overline{B(0,1)}$ by F_i is contained on $\Omega \cap G_i$, the lower half is in $\Omega^c \cap G_i$ and boundary of any of the halfs is in $\Gamma \cap G_i$, for all $i \in I$.*

Lipschitz domains are the ones that can locally parametrized by Lipschitz functions. In the same spirit, $\mathcal{C}^k$-domain are Lipschitz domains, where the condition (ii) is switched for:

$$F_i, F_i^{-1} \text{ are } \mathcal{C}^k(\Omega) \text{ maps.}$$

1.3.1. Functional Spaces

Basic tools for the analysis of partial differential equations are the notions of Banach and Hilbert spaces, in particular L^p spaces, and some key theorems such as Hahn-Banach theorem and open mapping theorem. Those topics are assumed to be known (Rudin, 2006).

In this work, all the functional spaces are be related to the Hilbert space $L^2(\Omega)$ with the usual interior product. For Lipschitz or $\mathcal{C}^k$-domains **n** denotes the outward normal of $\partial\Omega$, that is well defined and has components on $L^\infty(\Gamma)$ (Whitney, 2012).

Definition 1.2. *Let $f \in L^2(\Omega)$ for $i \in \{1 \dots d\}$. A class $\partial_{x_i} f$ of measurable functions differing only in a zero measure set, is called a weak derivative of f respect to x_i if*

$$(f, \partial_{x_i} g)_{L^2(\Omega)} = -(\partial_{x_i} f, g)_{L^2(\Omega)} \quad , \forall g \in \mathcal{C}_0^\infty(\Omega).$$

It is clear now that all the differential operators such as the gradient or divergence can be defined on a weak form. For a vector $\mathbf{m} \in \Pi_{i=1}^{d}\mathbb{N}$ and $f \in L^2(\Omega)$ the following differential operators can be defined:

$$\partial^{\mathbf{m}} f := \begin{cases} f & \mathbf{m} = \mathbf{0}, \\ \partial_{x_1}^{m_1} \dots \partial_{x_d}^{m_d} f & \mathbf{m} \neq \mathbf{0}. \end{cases}$$

Definition 1.3. *Let $n \in \mathbb{N}$. The space*

$$H^n(\Omega) := \{f \in L^2(\Omega) : \partial^{\boldsymbol{m}} f \in L^2(\Omega) \quad \forall \boldsymbol{m} \in \Pi_{i=1}^{d}\mathbb{N} : \|\boldsymbol{m}\|_\infty \leq n\},$$

is called a Sobolev space on Ω. Equivalently, the Sobolev spaces can be defined as the completion (or clausre) of $\mathcal{C}^\infty(\Omega)$ with the norm:

$$\|f\|_n^2 := \sum_{\alpha:\|\alpha\|_\infty \leq n} \|\partial^\alpha f\|_{L^2(\Omega)}^2.$$

Of great importance are the Sobolev spaces that result of the completion of $\mathcal{C}_0^\infty(\Omega)$ with the same norm. These spaces are denoted $H_0^n(\Omega) := \overline{\mathcal{C}_0^\infty(\Omega)}$.

REMARK 1.1. *For $f \in H^2(\Omega)$ the definition of Sobolev spaces implies:*

$$\partial^{\boldsymbol{p}} f \in L^2(\Omega) \quad \partial^{\boldsymbol{q}}\partial^{\boldsymbol{p}} f \in L^2(\Omega) \quad ,\forall(\boldsymbol{p},\boldsymbol{q}) : \|\boldsymbol{p}\|_\infty = \|\boldsymbol{q}\|_\infty = 1,$$

this means that $\partial^{\boldsymbol{p}} f \in H^1(\Omega) \quad \forall \boldsymbol{p} : \|\boldsymbol{p}\|_\infty = 1$. The result can be generalized in the following way, let $n \in \mathbb{N}, \boldsymbol{p} \in \Pi_{i=1}^{d}\mathbb{N} : \|\boldsymbol{p}\|_\infty \leq n$ and $f \in H^n(\Omega)$, then

$$\partial^{\boldsymbol{p}} f \in H^{n-\|\boldsymbol{p}\|_\infty}(\Omega). \tag{1.7}$$

For the definition of Sobolev spaces of non-integer order, it is necessary to introduce the notion of the norm of a non-integer derivative. Let $l \in (0,1)$ and $f \in L^2(\Omega)$ define the Sobolev $-$ Slobodeckii norm as:

$$|f|_l^2 := \int_\Omega \int_\Omega \frac{|f(\mathbf{x}) - f(\mathbf{y})|^2}{\|\mathbf{x} - \mathbf{y}\|^{d+2l}} d\mathbf{x} d\mathbf{y}.$$

For $s \in \mathbb{R}^+$, we split it as $s = \lfloor s \rfloor + l$, and then define the Sobolev space $H^s(\Omega)$ (resp. $H_0^s(\Omega)$) as the the completion of $\mathcal{C}^\infty(\Omega)$ (resp. $\mathcal{C}_0^\infty(\Omega)$) with the norm:

$$\|f\|_s^2 = \|f\|_{\lfloor s \rfloor}^2 + \sum_{\|\alpha\|_\infty \leq \lfloor s \rfloor} |\partial^\alpha f|_l^2.$$

PROPOSITION 1.1. *For $s \geq 0$, the Sobolev spaces $H^s(\Omega)$ are Hilbert spaces with interior product given by:*

$$(f,g)_{H^s} := \sum_{\|\alpha\|_\infty \leq \lfloor s \rfloor} (\partial^\alpha f, \partial^\alpha g)_{L^2(\Omega)} + \int_\Omega \int_\Omega \frac{(f(\boldsymbol{x}) - f(\boldsymbol{y}))\overline{(g(x) - g(y))}}{\|\boldsymbol{x} - \boldsymbol{y}\|^{d+2l}} d\boldsymbol{x} d\boldsymbol{y}.$$

The Sobolev spaces defined above, are all contained in $L^2(\Omega)$, this implies that theirs duals are going to contain the dual space of $L^2(\Omega)$. By the Riez theorem ((Sauter & Christoph, 2010) theorem 2.1.17), one can identify the dual space of $L^2(\Omega)$ with itself, in the sense that for all $G \in L^2(\Omega)'$ there is a unique $g \in L^2(\Omega)$ such that $G(f) = (f,g)_{L^2(\Omega)}$. Doing that the following inclusions hold:

$$H^{s_2}(\Omega) \subset H^{s_1}(\Omega) \subset L^2(\Omega) \subset (H^{s_1}(\Omega))' \subset (H^{s_2}(\Omega))',$$

where the action of an element of $(H^{s_2}(\Omega))'$ over one in $H^{s_2}(\Omega)$ is given by the bilinear form:

$$\langle f, g \rangle, \quad f \in (H^{s_2}(\Omega)) \quad , g \in (H^{s_2}(\Omega))',$$

named duality product, which is a continuous extension of the $L^2(\Omega)$-interior product. The dual of Sobolev spaces are denoted with negative index:

$$(H^s(\Omega))' = H_0^{-s}(\Omega),$$
$$(H_0^s(\Omega))' = H^{-s}(\Omega).$$

When the domain is not bounded the following spaces will be needed.

Definition 1.4. *For $s > 0$ and an open domain A*

$$H^s_{loc}(A) := \{f \in L^2_{loc}(A) : f|_U \in H^s(U) \quad \textit{for every open and bounded } U \subset A\} \quad (1.8)$$

Theorem 1.1. *(Sobolev Embedding Theorem)((Sauter & Christoph, 2010) theorem 2.5.4). If Ω is Lipschitz, then for $s > d/2$ the spaces $H^s(\Omega)$ can be continuously embedded* [4] *on $\mathcal{C}^0(\overline{\Omega})$. In the case in which Ω is a $\mathcal{C}^k$-domain then $H^s(\Omega)$ can be continuously embedded on $\mathcal{C}^m(\overline{\Omega})$ for $m < s - d/2$, and $s < k$.*

Finally, we define the Sobolev spaces over a manifold. [5]

Definition 1.5. *Let $k \in \mathbb{N}$ and $k < d$. A set $M \subset \mathbb{R}^d$ is called a k-dimensional manifold if there is a finite collection of subsets $\{M_i\}_{i\in I}$ and a set of bijective continuous maps, with continuous inverse $\{F_i : B(\boldsymbol{0}, 1) \mapsto M_i\}_{i\in I}$ such that, $\cup M_i = M$.*

For a manifold M a partition of the unity $\{\phi_i\}_{i\in I}$ of $\mathcal{C}^\infty_0$ functions such that :

$$\sum_{i\in I} \phi_i = 1, \quad \phi_i(x) = 0 \quad ,\forall x \in M\backslash M_i, \quad (1.9)$$

can be used to transform a function $f : M \mapsto \mathbb{R}$ onto a function $\tilde{f} : B(0, 1) \mapsto \mathbb{R}$ as

$$\tilde{f} := \sum_{i\in I} \tilde{f}_i,$$

$$\tilde{f}_i := (\phi_i \circ F_i)(f \circ F_i),$$

and then define the Sobolev norm:

$$\|f\|^2_{H^s(M)} := (\sum_{i\in I} \|\tilde{f}_i\|^2_{H^s(B(0,1))})^{1/2}.$$

With these tools, the Sobolev spaces can be defined on a manifold. In particular Sobolev spaces on Γ will play a major role in the next Section.

[4] This means that exist a continuous injective maps from $H^s(\Omega)$ on $\mathcal{C}^0(\overline{\Omega})$, or equivalently that every class of $H^s(\Omega)$ has a $\mathcal{C}^0(\overline{\Omega})$ representative

[5] In this thesis we will restrict to curves.

REMARK 1.2. *For manifolds such that $\partial M = \emptyset$* [6] *it can be show that*

$$H^s(M) = H_0^s(M) \quad s > 0.$$

Traditionally, for manifolds the space H_0^s is denoted $\tilde{H}^s(M)$, so in fact the duality relation for manifolds is denoted.

$$(H^s(M))' = \tilde{H}^{-s}(M),$$
$$(\tilde{H}^s(M))' = H^{-s}(M),$$

an equivalent definition for the spaces $\tilde{H}^s(M)$ will be given in the presentation of the multiple trace formulation.

1.3.2. Trace operator

Functional space setting, in particular Sobolev spaces, makes possible to extend the definition of the differential operators and formulate the partial differential equations in spaces with suitable properties. But the scattering problem also include conditions on the boundaries.

When the partial differential equation is considered with functions on $\mathcal{C}^k(\Omega)$ a condition of the form $f|_\Gamma$ is well defined because a continuous function can be evaluated on a zero measure set such as Γ, but when f is a class on a Sobolev space, the definition of the restriction is not clear.

Theorem 1.2. *((Sauter & Christoph, 2010) theorem 2.6.8). Let Ω be a Lipschitz domain, then for all $s \in (1/2, 3/2)$ exists two continuous linear operators:*

$$\gamma_D : H^s(\Omega) \to H^{s-1/2}(\Gamma),$$
$$\gamma_D^0 : H^s_{loc}(\Omega_0) \to H^{s-1/2}(\Gamma),$$

[6] The boundary of a manifold is defined as the image of $\partial B(0,1)$ by a continuous extension of the functions F_i.

such that if $f \in \mathcal{C}^0(\overline{\Omega}), and f_0 \in \mathcal{C}^0(\overline{\Omega_0})$ *are representants of a class on the Sobolev spaces, then*

$$\gamma_D f = f|_\Gamma,$$
$$\gamma_D^0 f_0 = f_0|_\Gamma.$$

The operator γ_D is called interior Dirichlet trace[7], this is in agreement with the condition $u|_\Gamma = g$ that is called Dirichlet condition. Also, the flux or Neumann trace can be defined on the Sobolev spaces as:

$$\begin{aligned} \gamma_N f &= (\mathbf{n}, \gamma_D \nabla f)_{\mathbb{R}^d}, \\ \gamma_N^0 f_0 &= (-\mathbf{n}, \gamma_D^0 \nabla f_0)_{\mathbb{R}^d}, \end{aligned}$$

where the interior (resp. exterior) Neumann trace is defined on $H^2(\Omega)$ (resp. $H^2_{loc}(\Omega_0)$), but it can be extended to a continuous linear operator between the following spaces:

$$\begin{aligned} \gamma_N : H^1(\Omega) &\rightarrow H^{-1/2}(\Gamma), \\ \gamma_N^0 : H^1_{loc}(\Omega_0) &\rightarrow H^{-1/2}(\Gamma). \end{aligned}$$

With the notion of traces, the whole scattering problem can be formulated on Sobolev spaces. Now the attention goes to the numerical method to solve it. Most of the numerical methods make use of the integration by parts formulas, this can also be done in Sobolev spaces, due to the density of the space $\mathcal{C}^\infty(\Omega)$. For seek completeness we present one result.

PROPOSITION 1.2. *((Sauter & Christoph, 2010) theorem 2.7.3). Let* Ω *be a Lipschitz domain and* $\boldsymbol{f} \in [H^1(\Omega)]^d$ *then:*

$$\int_\Omega div(\boldsymbol{f}) d\boldsymbol{x} = \int_\Gamma \boldsymbol{n} \cdot \gamma_D \boldsymbol{f} dS_{\boldsymbol{x}}. \tag{1.10}$$

[7] γ_d^0 is called exterior Dirichlet trace

1.3.3. Boundary element method

In this Section, we introduce the Boundary element method (shortened BEM) . The BEM, also called method of moments in some engineering literature, is a method to discretize partial differential equations similar to finite elements or finite differences. The main difference is that in BEM only degrees of freedom on the boundaries of the domains are defined, leading to much smaller linear systems. This characteristic make BEM suitable for problems where the domain is unbounded, but the boundary is finite. For example, in the direct scattering problem the domain is $\Omega \cup \Omega_0$ unbounded, but the boundary is only Γ.

The BEM is going to be introduced with a practical example, very similar to the scattering problem. Consider the problem to find $u : \mathbb{R}^2 \mapsto \mathbb{R}$ such that:

$$(-\Delta - \kappa_1^2)u(x,y) = 0 \qquad (x,y) \in \Omega, \tag{1.11}$$

$$(-\Delta - \kappa_0^2)u(x,y) = 0 \qquad (x,y) \in \Omega_0, \tag{1.12}$$

$$\gamma_D u(x,y) = \gamma_D^0 u(x,y) = g_D(x,y) \qquad (x,y) \in \Gamma, \tag{1.13}$$

$$+\text{radiation condition}, \tag{1.14}$$

where the domain Ω is assumed to be at least Lipschitz. Notice that this problem is unbounded because u has to be defined on Ω_0 . The key point for BEM is the representation theorem, it states that a function that fulfills the equations (1.11) and (1.12) can be reconstructed from its values at the boundary. Before present the theorem some tools are defined. To simplify the notation, the following auxiliary variables are introduced $\Omega_1 := \Omega$, $\gamma_D^1 := \gamma_D$ and $\gamma_N^1 := \gamma_N$.

Definition 1.6. *For $\kappa \in \mathbb{C}$, let $G_\kappa : \mathbb{R}^2 \times \mathbb{R}^2 \to \mathbb{R}$ given by*

$$G_\kappa(\boldsymbol{x},\boldsymbol{y}) = -\frac{i}{4} H_0^{(1)}(\kappa \|\boldsymbol{x} - \boldsymbol{y}\|), \tag{1.15}$$

is called the fundamental solution of the Helmholtz equation. Define the single layer and double layer potentials as

$$(S_i f)(\boldsymbol{x}) = \int_\Gamma G_{\kappa_i}(\boldsymbol{x},\boldsymbol{y}) f(\boldsymbol{y}) dS_{\boldsymbol{y}} \quad \boldsymbol{x} \notin \Gamma \quad \textit{Single layer potential}, \tag{1.16}$$

$$(D_i f)(\boldsymbol{x}) = \int_\Gamma \gamma_N^i G_{\kappa_i}(\boldsymbol{x},\boldsymbol{y}) f(\boldsymbol{y}) dS_{\boldsymbol{y}} \quad \boldsymbol{x} \notin \Gamma \quad \textit{Double layer potential}. \tag{1.17}$$

Theorem 1.3. *((Hiptmair & Jerez-Hanckes, 2012) theorem 2). The function u solves equations (1.11) , (1.12) and (1.14) if and only if it can be represented as:*

$$u|_{\Omega_i} = (D_i \gamma_D^i u)|_{\Omega_i} - (S_i \gamma_N^i u)|_{\Omega_i} \quad i \in \{0,1\}. \tag{1.18}$$

The next step is to obtain an equation that only involves the traces of u. For this the idea is to take traces at both sides of 1.18. This is not trivial because $G_\kappa(\mathbf{x},\mathbf{y})$ has a logarithmic singularity on $\mathbf{x} = \mathbf{y}$ and thus the potentials are not defined on Γ. Then we need assure the regularity of the potential in order to the trace be well defined.

PROPOSITION 1.3. *((Sauter & Christoph, 2010) theorem 3.1.16). For $s \in (-1/2, 1/2)$ and $i \in \{0,1\}$the following operators are linear and continuous:*

$$S_i : H^{-1/2+s}(\Gamma) \to H^{1+s}_{loc}(\mathbb{R}^2), \tag{1.19}$$

$$D_i : H^{1/2+s}(\Gamma) \to H^{1+s}_{loc}(\mathbb{R}^2 \backslash \Gamma). \tag{1.20}$$

Now the original problem is to find $u \in H^1_{loc}(\Omega_1 \cup \Omega_0)$ that fulfills (1.11)-(1.14) then due to theorem 1.2 the traces will have the following regularity:

$$\gamma_D^i u \in H^{1/2}(\Gamma), \tag{1.21}$$

$$\gamma_N^i u \in H^{-1/2}(\Gamma). \tag{1.22}$$

By the previous proposition and the regularity of the traces, the potentials have range on $H^{1+s}_{loc}(\mathbb{R}^2\backslash\Gamma)$. Then by the theorem 1.2 the traces of the Single layer and Double layer potentials are well defined and give rise to the so called boundary integral operators.

Definition 1.7. *For $i \in \{0,1\}$ the boundary integral operators V_i, K_i, K_i', W_i are defined as:*

$$V_i := \gamma_D^i S_i, \tag{1.23}$$

$$K_i := \gamma_D^i D_i - \frac{1}{2} Id, \tag{1.24}$$

$$K_i' := \gamma_N^i S_i + \frac{1}{2} Id, \tag{1.25}$$

$$W_i := -\gamma_N^i D_i. \tag{1.26}$$

Taking traces at both sides of (1.18) the following equations are obtained.

$$\gamma_D^i u = (K_i + \frac{1}{2} Id)\gamma_D^i u - V_i \gamma_N^i u, \tag{1.27}$$

$$\gamma_N^i u = -(W_i)\gamma_D^i u - (K_i' - \frac{1}{2} Id)\gamma_N^i u. \tag{1.28}$$

Notice that these equations are relations between the traces of u. If one of these equations is solved, the function can be reconstructed in every point of the space using the representation formula (1.18). Also, notice that the differential equation problem has been transformed into a integral equation problem. The boundary element method consists in discretizing (1.27) or (1.28) as in the finite element method. For example, since the Dirichlet trace is known by condition (1.13), replacing its value on (1.27) yields to the following equation for the Neumann trace:

$$V_i \gamma_N^i u = (K_i - \frac{1}{2} Id) g_D. \tag{1.29}$$

Consider now, a sequence of finite dimensional spaces $\{V_n\}_{n=1}^{\infty}$ such that $\cup_n V_n$ is dense on $H^{-1/2}(\Gamma)$ and for every $n \in \mathbb{N}$, an approximation of the Neumann trace can be written

in terms of $\{e_j^n\}_{j=1}^n$ a basis of V_n as:

$$u_n = \sum_{j=1}^{n} \alpha_j^n e_j^n. \tag{1.30}$$

The coefficients α_j^n can be obtained using a Galerkin variational scheme. This means, that instead of imposing equation (1.29) as elements of $H^{1/2}(\Gamma)$, they have to be equal when tested with any element of the dual space[8] $\tilde{H}^{-1/2}(\Gamma)$ (the same that $H^{-1/2}(\Gamma)$ because Γ is a closed curve). At the continuous level give rise to the following equation:

$$\langle V_i \gamma_N^i u, \phi \rangle = \langle (K_i - \frac{1}{2} Id) g_D, \phi \rangle \quad , \forall \phi \in H^{-1/2}(\Gamma). \tag{1.31}$$

At the discrete level, $\gamma_N^i u$ is changed for the approximation u_n, and the elements of the base of V_n are used as test [9]. Then we get the following square linear system:

$$\sum_{j=1}^{n} \alpha_j^n \langle V_i e_j^n, e_k^n \rangle = \langle (K_i - \frac{1}{2} Id) g_D, e_k^n \rangle \quad \forall k \in \{1 \dots n\}. \tag{1.32}$$

REMARK 1.3. *We mention a few relevant points on BEM.*

(i) *Notice that u_n is an approximation of the interior or exterior Neumann trace depending of the value of $i \in \{0, 1\}$ in (1.32).*

(ii) *If each space V_n is chosen such that $V_n \subset L^2(\Gamma)$,then the duality products on (1.32) are reduced to internal products on $L^2(\Gamma)$.*

(iii) *Many difficulties related to BEM are not clear from this presentation. For example, the computation of the boundary integral operators implies computing integrals of singular functions. Also, the linear system that arise of the discretization of (1.27) or (1.28) involes a dense matrix. There exist techniques to tackle these difficulties (Bebendorf, 2008) but this topic is out of the scope of this introduction.*

[8] This two conditions are equivalent due to Hahn-Banach Theorem.

[9] They take the role of ϕ on (1.31).

(iv) *In order to establish that in fact there is convergence* $u_n \to \gamma_N^0 u$ *or* $u_n \to \gamma_N^1 u$ *as well as the existence and uniqueness of the solutions* u_n.

This finish the presentation of boundary element method, the next subSection introduces a method for solving linear systems that is commonly used for BEM, but is mostly independent of the previous subSections.

1.4. Linear system solver

Let $A \in \mathbb{R}^{n\times n}$ be an invertible matrix and $\mathbf{b} \in \mathbb{R}^n$. The focus of this Section is to present some tools to find the solution $\mathbf{x} \in \mathbb{R}^n$ of the linear system

$$A\mathbf{x} = \mathbf{b}. \tag{1.33}$$

The main reference for this topic is (Saad, 2003).

1.4.1. Generalized Minimum Residual Method

Let $\{\mathcal{K}\}_{m=1}^n$ be a sequence of subspaces of $\mathbb{R}^n$ such that $\dim(\mathcal{K}_m) = m$. The Generalized Minimum Residual Method (shortened GMRES) is an iterative method that, in each step constructs an approximation $\mathbf{x}_m \in \mathcal{K}_m$ of the solution $\mathbf{x}$ of (1.33), such that the norm of the residual $\mathbf{b} - A\mathbf{x}_m$ is minimized. Before introduce more details of the method, a basic result on Hilbert spaces is recalled.

Theorem 1.4. *((Saad, 2003) theorem 1.38). Let* H *be a Hilbert space with interior product* $(,)_H$ *and* S *a subspace of* H. *Then for* $x \in H$ *and* $x_s \in S$ *the following affirmations are equivalent:*

(i)

$$\min_{s\in S} \|x - s\| = \|x - x_s\|, \tag{1.34}$$

(ii)

$$(x - x_s, s)_H = 0 \quad , \forall s \in S, \tag{1.35}$$

and the solution x_s is unique.

If the theorem 1.4 is applied to find $\min \|\mathbf{b} - A\mathbf{v}\| = \min_{\mathbf{u} \in A\mathcal{K}_m} \|\mathbf{b} - \mathbf{u}\|$, the equivalent condition is:

$$(\mathbf{b} - A\mathbf{x}_m, \mathbf{u})_{\mathbb{R}^n} = 0 \quad , \forall \mathbf{u} \in A\mathcal{K}_m. \tag{1.36}$$

The direct method to solve (1.36) would be to use a base for the space $\mathcal{K}_m$ and get a $m \times m$ linear system. Obviously, this is not optimum, since implies to solve another linear system. There are other techniques to solve (1.36) most of them are based on obtaining an orthonormal base of $\mathcal{K}_m$ and then the problem can be solved easily, the technique used will depend of the implementation of the GMRES.

The space $\mathcal{K}_m$ is defined for a initial vector $\mathbf{x}_0$ and residual $\mathbf{r}_0 := \mathbf{b} - A\mathbf{x}_0$ as :

$$\mathcal{K}_m = \text{span}\{\mathbf{r}_0, A\mathbf{r}_0, \dots A^{m-1}\mathbf{r}_0\}. \tag{1.37}$$

The advantage of GMRES over a direct solver is that it requires less arithmetic operations per iteration and thus can solve much bigger systems. Also, the GMRES performance can be boosted with the inclusion of some hierarchical matrix techniques (Bebendorf, 2008). In comparison to others iterative solvers, the main advantage is that GMRES can be applied to any matrix A, it does not relay on a special structure such as Hermitian matrix or positive defined. On the down side, GMRES can have a very slow convergence, and in some basic implementations, requires a large amount of memory if convergence is not fast[10]. Some implementations use a restart, which means that have a fixed limit of number of vectors to store and when reached it restart subspaces with the new $\mathcal{K}_0$ given by the last solution found, however this can broke the entire convergence of the method.

[10]Because it has to store the basis of the entire $\mathcal{K}_m$.

It is well known that the GMRES produces a sequence of monotonic decreasing residuals that converge to the solution of the linear system, but it is not clear how fast it converges for a general matrix A.

In particular cases there are results like the following:

PROPOSITION 1.4. *((Saad, 2003) Section 6.11.4). If A is positive definite and $\boldsymbol{r}_n := \boldsymbol{b} - A\boldsymbol{x}_m$ then*

$$\|\boldsymbol{r}_m\| \leq \left(1 - \frac{\lambda^2_{\min}(1/2(A^T + A))}{\lambda_{\max}(A^T A)}\right)^{m/2} \|\boldsymbol{r}_0\|, \tag{1.38}$$

where λ_{max} denotes the maximum eigenvalue and λ_{min} is the minimum.

The previous result and also numerical experiments has shown that the convergence of GMRES is determined by the spectral properties of the matrix A. Even if the properties imply a slow convergence, the linear system can be changed for other one that is equivalent, but has better behavior, which is the topic of the next Section.

1.4.2. Preconditioners

As stated before, the performance of GMRES depends of spectral properties of the matrix A. In fact, the performance of GMRES and any other iterative or method, depends of the condition number of the matrix, that can be defined as: (1.39).

$$cond_2(A) := \frac{|\lambda_{max}|}{|\lambda_{min}|}. \tag{1.39}$$

A high condition number implies that the linear system is hard to solve, and poor performance of the iterative methods. The condition number of a matrix can be changed if it is multiplied for for a non singular matrix. For example if A^{-1} is known then:

$$cond_2(A^{-1}A) = cond_2(AA^{-1}) = 1. \tag{1.40}$$

This is an ideal situation because, if A^{-1} is known there is not need to use any iterative method. Sometimes there is a matrix $P_r \in \mathbb{R}^{n\times n}$ or $P_l \in \mathbb{R}^{n\times n}$ such that P_lA or AP_r have a better condition number than A. In these cases, instead of solving (1.33), one of the following alternative systems can be solved:

$$(P_lA)\mathbf{x} = (P_l\mathbf{b}), \tag{1.41}$$

$$(AP_r)\mathbf{y} = \mathbf{b} \quad P_r\mathbf{y} = \mathbf{x}, \tag{1.42}$$

the matrix P_r is called *right preconditioner* and P_l is called *left preconditioner*.

1.5. Objectives

The main objective of this thesis, is to extend the multiple traces formulation [11] for the use of spectral basis of approximations, and then leading to a formulation able to tackle hight frequency problems. Aside from the theory concerning the model is expected to have a numerical implementation that can validate the results for cases where the analytical solution is knowm.

[11] The multiple trace formulation will be introduced on chapter 2.

2. LOCAL MULTIPLE TRACES FORMULATION FOR HIGH-FREQUENCY SCATTERING PROBLEMS

2.1. Introduction

Many areas in engineering ranging from biomedical imaging via ultrasound or electromagnetic waves to the design of antennae and telescopes, greatly profit from the ever-increasing computational processing capacity to simulate wave scattering. After decades of development, Boundary Integral (BI)-based techniques (Sauter & Christoph, 2010), also known as the Method of Moments (MoM), have rightfully gained their place among the modeling tools available for mathematicians, physicists and engineers. By employing the appropriate Green's functions, these methods portray wave propagation in the entire unbounded homogeneous space by solving first or second kind Fredholm boundary integral equations (BIEs) on the surface of the scatterers. However, in most realistic scenarios, e.g., whenever scatterers are composed of several distinct parts of largely different sizes, standard discretization of the BIEs leads to large dense linear systems for which existing iterative solving algorithms perform poorly. Indeed, a fixed number of degrees of freedom is mandatory per wavelength in order to represent oscillatory solutions quickly leading to prohibitive computational expenses. Moreover, the conditioning number of the matrices obtained can be shown to increase with the wavenumber.

Several solution strategies have been proposed to deal with this so-called *high frequency* problem. One approach seeks to find faster implementations of standard methods, such as fast multipole methods (Darve & Havé, 2004a, 2004b; Darrigrand, 2002; Chen & Chiu, 2002). Another body of work relies on asymptotic techniques such as geometrical optics, physical optics and the geometrical theory of diffraction (Lin, 2014; Philbin, 2014). Such approximations are computationally cheap but generally accurate only for sufficiently high frequencies. Hence, questions arise as to when and how these techniques should be applied and what to do in situations that require accommodating different ranges

of frequencies as in the case of highly contrasting materials (heterogenous scatters). Taking a different direction, and perhaps closer to our work, Bruno and co-workers (Bruno & Reitich, 2008; Bruno & Lintner, 2013) have solved the arising high-frequency BIEs using spectral techniques for Nyström methods for perfectly conducting scatterers.

As it usually happens, algorithm hybridization may bring the best of worlds. More precisely, one seeks to incorporate asymptotic information of the highly oscillatory nature of the problem into the approximation space, yielding *Hybrid Numerical-Asymptotic* methods (de La Bourdonnaye, 1994; Chandler-Wilde, Graham, Langdon, & Spence, 2012; Hewett, Langdon, & Melenk, 2013; Domínguez, Graham, & Smyshlyaev, 2007; Ecevit & Reitich, 2009; Anand, Boubendir, Ecevit, & Reitich, 2010). Although most of these efforts focus on impenetrable scatterers, Groth *et al.* (Samuel P. Groth, 2013) have recently proposed an adaptation of the HNA approach to deal with a single penetrable object but the extension to heterogeneous scatterers is unclear.

Hence, the question remains: is it possible to solve scattering problems for heterogeneous objects portraying a large frequency range in practical terms? To answer this, we will follow the spirit of the *Multiple Traces Formulations* (MTFs) (Hiptmair & Jerez-Hanckes, 2012; Claeys, Hiptmair, & Jerez-Hanckes, 2013; Claeys & Hiptmair, 2013; Claeys, Hiptmair, Jerez-Hanckes, & Pintarelli, 2014) and tackle two-dimensional composite scatterers with largely varying wavenumbers. In particular, we will focus on a variant dubbed *local* since all unknown boundary traces and test functions are locally defined on subdomain boundaries. As a Galerkin-Petrov formulation, transmission conditions are enforced weakly by testing with also locally defined test functions. On the continuous level, the resulting first-kind Fredholm equation possesses unique solutions. Hence, the formulation is more robust than other formulations, as it naturally rejects spurious resonances, i.e. non-trivial but unphysical solutions for certain exterior wavenumbers. Moreover, the resulting block diagonal structure hints at its amenability to parallelization and operator

preconditioning. Numerical analysis and results in two and three dimensions already validated this for low-order elements. However, and as expected, such discretization bases are not sufficient for high-frequency regimes, and so we will explore a purely *spectral* or p-refinement approximation for boundary unknowns. In doing so, we will further extend the mathematical formalism provided for the local MTF to account for piecewise Cauchy data and show that the formulation lends itself to preconditioning quite easily.

Outline. In Section 2.2 we recall and generalize the derivation of local MTF for piecewise traces, which requires imposing Calderón identities weakly. Readers may skip technical subsections 2.2.1, 2.2.3, 2.2.4 to check the final formulation in 2.2.5. Spectral discretization will be carried out using Chebyshev polynomials as shown in Section 2.3. There we present the numerical analysis required for deducing existence and uniqueness on the discrete level as well as bounds on the errors based on projection estimates over weighted Sobolev spaces. Moreover, we discuss the efficient implementation using fast Fourier techniques (FFT). Numerical results portraying the efficiency and power of the method proposed, are introduced in Section 2.4 for the simple setting of a circle divided in two halves. This configuration already present the difficulties inherent to the problem: triple points and different wavenumbers. Particular attention is given to error convergence and to the effect of diagonal preconditioning on iterative solvers as shown in Section 2.4.5. Conclusions and future directions are drawn in section 2.5.

2.2. Generalized Local Multiple Traces Formulation

2.2.1. Functional spaces

Let $\mathcal{O}$ be a bounded closed domain. We denote by $L^p(\mathcal{O})$, $\mathcal{D}(\mathcal{O})$, $\mathcal{D}'(\mathcal{O})$ and $H^s(\mathcal{O})$, the standard Lebesgue space for $p \in [1, \infty]$, the space of C^∞-compactly supported functions, the space of distributions, and Sobolev spaces for $s \geq 0$, respectively, all defined over $\mathcal{O}$ (McLean, 2000). If $\mathcal{O}$ has a boundary, we assume that it can be extended to a

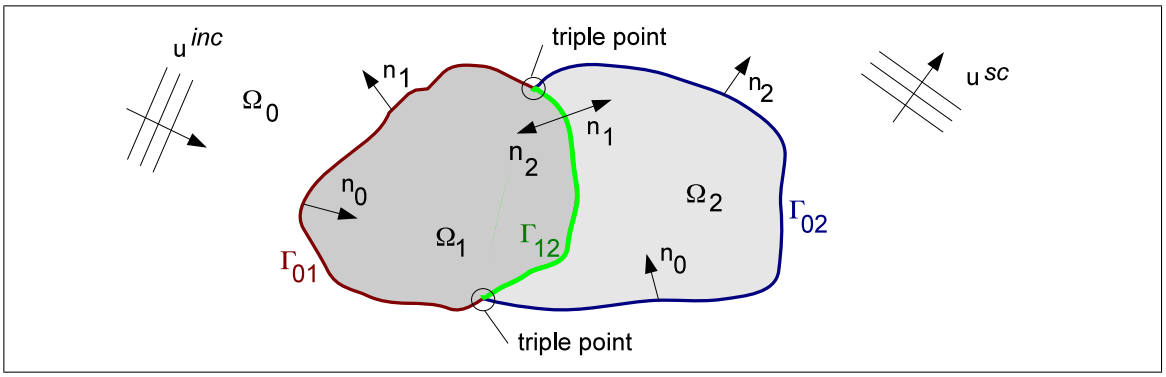

Figure 2.1. Simple model geometry. Observe normal definitions.

closed manifold $\widetilde{\mathcal{O}}$, with $\mathcal{O} \subset \widetilde{\mathcal{O}}$, and write $\widetilde{u}$ for the extension of u by zero over $\widetilde{\mathcal{O}}$. For $s > 0$ and $\mathcal{O}$ Lipschitz, one defines the closed subspace of $\widetilde{H}^s(\mathcal{O})$:

$$\widetilde{H}^s(\mathcal{O}) := \{u \in H^s(\mathcal{O}) \,:\, u \in H^s(\widetilde{\mathcal{O}})\} \tag{2.1}$$

provided with the norm $\|u\|_{\widetilde{H}^s(\mathcal{O})} = \|\widetilde{u}\|_{H^s(\widetilde{\mathcal{O}})}$, where the last norm is the standard one. For $s < 0$ we use the L^2-duality product so that $\widetilde{H}^s(\mathcal{O})$ is the dual of $H^{-s}(\mathcal{O})$. We will be particularly interested in

$$\widetilde{H}^{-1/2}(\mathcal{O}) = \big(H^{1/2}(\mathcal{O})\big)' \quad \text{and} \quad H^{1/2}(\mathcal{O}) = \Big(\widetilde{H}^{1/2}(\mathcal{O})\Big)'. \tag{2.2}$$

2.2.2. Model problem

Without loss of generality, we consider the geometric arrangement shown in Figure 2.1 where $\Omega := \bar{\Omega}_1 \cup \bar{\Omega}_2$ is a heterogenous simply connected scatterer, composed of two bounded simply connected subdomains $\Omega_1, \Omega_2 \in \mathbb{R}^2$. The exterior domain is denoted by $\Omega_0 := \mathbb{R}^2 \setminus \bar{\Omega}$ and interfaces by $\Gamma_{ij} := \partial\Omega_i \cap \partial\Omega_j$. We will make use of the index set $\Lambda_i = \{j \in \mathbb{N} : \partial\Omega_i \cap \partial\Omega_j \neq \emptyset\}$ for $i = 0, 1, 2$.

For an exciting plane wave u^{inc}, we seek u representing the field scattered in Ω_0 and total field in Ω which satisfy homogeneous Helmholtz equations, with constant wavenumbers $\kappa_i \in \mathbb{C} \setminus \mathbb{R}_-$ in each subdomain $\Omega_i, i = 0, 1, 2$. Explicitly, we seek $u \in H^1_{\text{loc}}(\Omega \cup \Omega_0)$

such that

$$-\Delta u - \kappa_i^2 u = 0, \qquad \forall\, \mathbf{x} \in \partial\Omega_i, \quad i = 0, 1, 2, \tag{2.3a}$$

$$[\boldsymbol{\gamma} u] = \mathbf{g}, \qquad \forall\, \mathbf{x} \in \Gamma_{01} \cup \Gamma_{02}, \tag{2.3b}$$

$$[\boldsymbol{\gamma} u] = \mathbf{0}, \qquad \forall\, \mathbf{x} \in \Gamma_{12}, \tag{2.3c}$$

$$+\,\text{radiation conditions} \qquad \text{when } \|\mathbf{x}\| \to \infty. \tag{2.3d}$$

Here we have used the notation $\boldsymbol{\gamma}^i := (\gamma_D^i, \gamma_N^i)$ for standard Dirichlet and Neumann interior traces on subdomain boundary $\partial\Omega_i$, so that (2.3b) and (2.3c) represent inhomogeneous, $\mathbf{g} = -\boldsymbol{\gamma} u^{\text{inc}} \in H^{1/2}(\partial\Omega_i) \times H^{-1/2}(\partial\Omega_i)$, and homogenous transmission conditions, respectively, with $[\cdot]$ denoting trace jump across the indicated interface.

2.2.3. Weak transmission conditions

We now extend the local MTF to spectral elements as in (Hiptmair & Jerez-Hanckes, 2012). Such elements will be defined per interface Γ_{ij}, so instead of working on standard functional spaces $\mathbf{V}_i := H^{1/2}(\partial\Omega_i) \times H^{-1/2}(\partial\Omega_i)$, we will rely on "broken" spaces:

$$\mathbf{V}_i^{\text{pw}} := H_{\text{pw}}^{1/2}(\partial\Omega_i) \times H_{\text{pw}}^{-1/2}(\partial\Omega_i), \quad \widetilde{\mathbf{V}}_i := \widetilde{H}_{\text{pw}}^{1/2}(\partial\Omega_i) \times \widetilde{H}_{\text{pw}}^{-1/2}(\partial\Omega_i), \tag{2.4}$$

where

$$H_{\text{pw}}^{\pm 1/2}(\partial\Omega_i) := \{u \in \mathcal{D}'(\partial\Omega_i) : u|_{\Gamma_{ij}} \in H^{\pm 1/2}(\Gamma_{ij}), \forall\, j \in \Lambda_i\}, \tag{2.5}$$

and similarly for $\widetilde{H}_{\text{pw}}^{\pm 1/2}(\partial\Omega_i)$. Observe that $\mathbf{V}_i^{\text{pw}}$ and $\widetilde{\mathbf{V}}_i$ are dual to each other when taking the cross duality product between cartesian elements $\langle \cdot\,, \cdot \rangle_\times$, e.g., $\langle \boldsymbol{\lambda}^i\,, \boldsymbol{\varphi}^j \rangle_\times := \langle \lambda_{\text{D}}^i\,, \boldsymbol{\varphi}_{\text{N}}^j \rangle + \langle \lambda_{\text{N}}^i\,, \varphi_{\text{D}}^j \rangle$.

Transmission conditions are weakly enforced across each interface Γ_{ij}. This is done via local restriction and normal orientation operators, such that adjacent normals are reoriented. Then, extension by zero onto the adjacent subdomain boundary is required

to set up a single subdomain boundary equation. For this, we make use of *restriction-orientation-and-extension operators*, $\widetilde{\mathsf{X}}_{ij}$ mapping $\mathbf{V}_j^{\text{pw}} \to \mathbf{V}_i^{\text{pw}}$ when defined in duality with $\widetilde{\widetilde{\mathbf{V}}}_i$.

2.2.4. Weak Calderón identities

We define our unknowns on subdomains Ω_i as $\boldsymbol{\lambda}^i := (\lambda_D^i, \lambda_N^i) \in \mathbf{V}_i^{\text{pw}}$. Notice that these are not strictly Cauchy data. However, we can weakly enforce Calderón identities satisfied by each unknown locally. More specifically, integral representations in each subdomain are used to set up Calderón identities over boundaries $\partial\Omega_i$, such that for all $\boldsymbol{\varphi} \in \widetilde{\widetilde{\mathbf{V}}}_i$ it holds

$$\begin{aligned}
\left\langle \boldsymbol{\lambda}^i \,,\, \boldsymbol{\varphi}^i \right\rangle_{\times} &= \left\langle \left(\frac{1}{2}\mathrm{Id} + \mathsf{A}_i \right) \boldsymbol{\lambda}^i \,,\, \boldsymbol{\varphi}^i \right\rangle_{\times} \\
&= \left\langle \begin{pmatrix} \frac{1}{2}\mathrm{Id} - \mathsf{K}_i & \mathsf{V}_i \\ \mathsf{W}_i & \frac{1}{2}\mathrm{Id} + \mathsf{K}_i' \end{pmatrix} \begin{pmatrix} \lambda_{\mathrm{D}}^i \\ \lambda_{\mathrm{N}}^i \end{pmatrix} , \begin{pmatrix} \varphi_{\mathrm{D}}^i \\ \varphi_{\mathrm{N}}^i \end{pmatrix} \right\rangle_{\times} ,
\end{aligned}$$

where $\mathsf{A}_i : \mathbf{V}_i \to \mathbf{V}_i$ contains the standard weakly singular, double layer, adjoint double layer and hypersingular integral operators, denoted $\mathsf{V}_i, \mathsf{K}_i, \mathsf{K}_i'$ and W_i, respectively, over $\partial\Omega_i$ for a wavenumber $\kappa_i > 0$ and fundamental solution (Sauter & Christoph, 2010):

$$G_i(\mathbf{x}, \mathbf{y}) := \frac{\imath}{4} H_0^{(1)}(\kappa_i \left\| \mathbf{x} - \mathbf{y} \right\|_2) \tag{2.6}$$

where $H_0^{(1)}(\cdot)$ is the zeroth order Hankel function of the first kind.

2.2.5. Final formulation

Define $\mathbb{V}^{\text{pw}} := \prod_{i=0}^{2} \mathbf{V}_i^{\text{pw}}$ and $\widetilde{\widetilde{\mathbb{V}}} := \prod_{i=0}^{2} \widetilde{\widetilde{\mathbf{V}}}_i$. With the above, the variational form of the MTF system is to seek $\boldsymbol{\lambda} = (\boldsymbol{\lambda}^0, \boldsymbol{\lambda}^2, \boldsymbol{\lambda}^2) \in \mathbb{V}^{\text{pw}}$, such that for all $\boldsymbol{\varphi} = (\boldsymbol{\varphi}^0, \boldsymbol{\varphi}^1, \boldsymbol{\varphi}^2) \in \widetilde{\widetilde{\mathbb{V}}}$

it holds

$$\langle \mathsf{M}\boldsymbol{\lambda}\,,\,\boldsymbol{\varphi}\rangle = \left\langle \mathsf{M}\begin{pmatrix}\boldsymbol{\lambda}^0\\ \boldsymbol{\lambda}^1\\ \boldsymbol{\lambda}^2\end{pmatrix}\,,\,\begin{pmatrix}\boldsymbol{\varphi}^0\\ \boldsymbol{\varphi}^1\\ \boldsymbol{\varphi}^2\end{pmatrix}\right\rangle_{\times} = \left\langle \begin{pmatrix}\mathbf{g}^0\\ \mathbf{g}^1\\ \mathbf{g}^2\end{pmatrix}\,,\,\begin{pmatrix}\boldsymbol{\varphi}^0\\ \boldsymbol{\varphi}^1\\ \boldsymbol{\varphi}^2\end{pmatrix}\right\rangle_{\times} \tag{2.7}$$

where

$$\mathsf{M} := \begin{pmatrix} \mathsf{A}_0 & -\frac{1}{2}\widetilde{\mathsf{X}}_{01} & -\frac{1}{2}\widetilde{\mathsf{X}}_{02}\\ -\frac{1}{2}\widetilde{\mathsf{X}}_{10} & \mathsf{A}_1 & -\frac{1}{2}\widetilde{\mathsf{X}}_{12}\\ -\frac{1}{2}\widetilde{\mathsf{X}}_{20} & -\frac{1}{2}\widetilde{\mathsf{X}}_{21} & \mathsf{A}_2 \end{pmatrix}. \tag{2.8}$$

with A_i again denoting block boundary integral operators per subdomain and $\widetilde{\mathsf{X}}_{ij}$ taking care of transmission conditions per interface.

Structurally, the MTF is amenable to parallelization as each subdomain operator can be sent to different thread. Compared to the original version (Hiptmair & Jerez-Hanckes, 2012), the difference lies in that the new Galerkin-Petrov system requires local test functions to have restrictions to interfaces Γ_{ij} lying in $\widetilde{H}^{1/2}(\Gamma_{ij}) \times \widetilde{H}^{-1/2}(\Gamma_{ij})$. In practical terms: Dirichlet traces have to become zero at triple points for 2D, while for Neumann data standard bases can be used.

THEOREM 1 (Existence and Uniqueness). *The local MTF system* (2.7) *has a unique solution in* $\mathbb{V}^{pw}$ *for all* $\mathbf{g}$ *in* $\mathbf{V}_0$.

PROOF. This result follows from the same statement for $\mathbb{V} := \prod_{i=0}^{2} \mathbf{V}_i$ in (Hiptmair & Jerez-Hanckes, 2012). Extension to piecewise spaces is achieved by duality pairings. □

2.3. Discretization by Spectral Elements

2.3.1. Preliminaries

Define the characteristic function $\mathbf{1}_{\mathcal{O}}$ of a set $\mathcal{O}$ of non-zero measure:

$$\mathbf{1}_{\mathcal{O}}(t) = \begin{cases} 1 & \text{if } t \in \mathcal{O}, \\ 0 & \text{if } t \in \mathcal{O}^c. \end{cases} \tag{2.9}$$

Set $\hat{\Gamma} := [-1, 1]$. We assume that for each interface Γ_{ij} there is a C^1-parametri-zation of $\hat{\Gamma}$. Since we assume simply connected domains Ω_i, the union of interfaces renders $\partial\Omega_i$ a closed curved Lipschitz surface. Specifically, for a subdomain boundary $\partial\Omega_i$, we set $h_{ij} : \hat{\Gamma} \to \Gamma_{ij}$ as a positive oriented parametrization of Γ_{ij}. Similarly, we define over $\partial\Omega_j$, a parametrization $h_{ji} : \hat{\Gamma} \to \Gamma_{ij}$. These two parameterizations are required in order to properly orientate subdomains' normals. However, as we will later see, the positive orientation requirement can be dropped as h_{ij}, h_{ji} will be used solely to compute scalar line integrals.

2.3.2. Spectral Elements – Chebyshev polynomials

We will discretize (2.7) using as both trial and test functions Chebyshev polynomials defined over the parameter space $\hat{\Gamma}$ and mapped over each interface Γ_{ij}. The Chebyshev polynomials $T_m(x)$ and $U_m(x)$ of the first and second kinds, respectively, are polynomials of degree $m \in \mathbb{N}$, defined in $x \in \hat{\Gamma}$ as:

$$T_m(x) \;=\; \cos m\theta \qquad \text{and} \qquad U_m(x) \;=\; \frac{\sin\left(m+1\right)\theta}{\sin\theta} \tag{2.10}$$

with $x = \cos\theta$. These satisfy the recurrence relation (Abramowitz, 1988, Form. 2.3.14, 2.3.16) :

$$P_m(x) \;=\; 2xP_{m-1}(x) \;-\; P_{m-2}(x)\,, \quad m \;=\; 2, 3, \ldots, \tag{2.11}$$

together with initial conditions $T_0(x) = 1$, $T_1(x) = x$, $U_0(x) = 1$ and $U_1(x) = 2x$. Furthermore, it holds for $m \in \mathbb{N}$

$$U_m(x) - U_{m-2}(x) = 2T_m(x), \quad m \geq 2, \tag{2.12}$$

$$T'_m(x) = n\, U_{m-1}(x)\,, \tag{2.13}$$

$$(\omega(x)U_{m-1}(x))' = -\, m\omega^{-1}(x)T_m(x), \tag{2.14}$$

where the weight function $\omega(x)$ is given by

$$\omega(x) := \sqrt{1 - x^2}, \qquad \text{for } x \in \hat{\Gamma}. \tag{2.15}$$

Moreover, the T_m are orthogonal with respect to ω^{-1}:

$$\int_{-1}^{1} T_n(x)\, T_m(x)\, \omega^{-1}(x)\, dx = \begin{cases} 0, & n \neq m\,, \\ \pi/2, & n = m \neq 0\,, \\ \pi, & n = m = 0\,. \end{cases} \tag{2.16}$$

For the second kind Chebyshev polynomials U_m, it holds

$$\int_{-1}^{1} U_n(x)\, U_m(x)\, \omega(x)\, dx = \begin{cases} 0, & n \neq m, \\ \pi/2, & n = m \neq 0. \end{cases} \tag{2.17}$$

Based on the above, we will construct trial and test function bases for the MTF (2.7) as piecewise combinations of Chebyshev polynomials mapped over interfaces Γ_{ij}. For this, we first define canonical bases for trial and test elements restricted over the reference segment $\hat{\Gamma}$, denoted $\hat{\mathbb{T}}_L := \operatorname{span}\{\hat{\boldsymbol{\lambda}}_l\}_{l=0}^{L}$ and $\hat{\mathbb{Q}}_L := \{\hat{\boldsymbol{\varphi}}_l\}_{l=0}^{L}$, respectively, for any $L \in \mathbb{N}$, in the following fashion:

$$\hat{\boldsymbol{\lambda}}_l := (\hat{\lambda}_{\mathrm{D},l}, \hat{\lambda}_{\mathrm{N},l}) = (T_l, U_l) \quad \text{and} \quad \hat{\boldsymbol{\varphi}}_l = (\hat{q}_l, \hat{q}_l), \quad \hat{q}_l := \omega U_l, \quad \forall\, l \in \mathbb{N}_0, \tag{2.18}$$

and where the weight ω forces $\hat{q}_l$ to vanish at the endpoints of $\hat{\Gamma}$. We need to show that sequences generated by $\hat{\mathbb{T}}_L$ and $\hat{\mathbb{Q}}_L$ are dense in $H^{1/2}(\hat{\Gamma}) \times H^{-1/2}(\hat{\Gamma})$ and $\widetilde{H}^{1/2}(\hat{\Gamma}) \times \widetilde{H}^{-1/2}(\hat{\Gamma})$, respectively. For this, we first introduce the next auxiliary lemma.

LEMMA 1. *Let $f \in L^\infty(\hat{\Gamma})$ and $\delta > 0$. There exists $f_1^\delta \in L^\infty(\hat{\Gamma})$ such that*

$$\left\| f - \omega f_1^\delta \right\|_{L^2(\hat{\Gamma})} \leq \delta. \tag{2.19}$$

PROOF. Let $\epsilon > 0$ and define $f_1^\epsilon := \omega^{-1} f \mathbf{1}_{\omega > \epsilon} \in L^\infty(\hat{\Gamma})$ and $f_2^\epsilon := f \mathbf{1}_{\omega \leq \epsilon}$. Clearly, $f = \omega f_1^\epsilon + f_2^\epsilon$ and it holds

$$\| f - \omega f_1^\epsilon \|_{L^2(\hat{\Gamma})} = \| f_2^\epsilon \|_{L^2(\hat{\Gamma})} \leq \sqrt{2\epsilon} \, \| f \|_{L^\infty(\hat{\Gamma})} . \tag{2.20}$$

Then it suffices to take $\epsilon = \dfrac{\delta^2}{2 \| f \|_{L^\infty}^2}$ to obtain the desired result. □

PROPOSITION 2.1. *The sequence of subspaces $\{\hat{\mathbb{T}}_L\}_{L \in \mathbb{N}}$ is dense in $H^{1/2}(\hat{\Gamma}) \times H^{-1/2}(\hat{\Gamma})$ and $\{\hat{\mathbb{Q}}_L\}_{L \in \mathbb{N}}$ in $\widetilde{H}^{1/2}(\hat{\Gamma}) \times \widetilde{H}^{-1/2}(\hat{\Gamma})$.*

PROOF. Density of subspaces $\{\hat{\mathbb{T}}_L\}_{L \in \mathbb{N}}$ in $H^{1/2}(\hat{\Gamma}) \times H^{-1/2}(\hat{\Gamma})$ follows from the density of polynomials onto the space of continuous functions (Weierstrass' theorem), and by invoking Sobolev embeddings (Sauter & Christoph, 2010, Section 2.5). Hence, we focus on proving the statement for $\hat{\mathbb{Q}}_L$ for which we focus on the properties of $\hat{Q}_L := \operatorname{span}\{\hat{q}_l\}_{l=0}^L$. That $\hat{Q}_L$ is dense in $\widetilde{H}^{1/2}(\hat{\Gamma})$ follows from Chebyshev expansion and density results (Jerez-Hanckes & Nédélec, 2012, Sect. 4.5). Thus, we are left to tackle the density $\hat{Q}_L$ in $\widetilde{H}^{-1/2}(\hat{\Gamma})$.

Let $\epsilon > 0$ and $f, g \in \mathcal{D}(\hat{\Gamma})$. By density arguments, it is sufficient to show that there exists an $L \in \mathbb{N}$ such that for a certain $f_L \in \hat{Q}_L := \operatorname{span}\{\hat{q}_l\}_{l=0}^L$ it holds

$$\| f - f_L \|_{\widetilde{H}^{-1/2}(\hat{\Gamma})} = \sup_{g \in \mathcal{D}(\hat{\Gamma})} \frac{\langle f - f_L \, , \, g \rangle}{\| g \|_{H^{1/2}(\hat{\Gamma})}} \leq \epsilon. \tag{2.21}$$

Since $f_L \in Q_L$, $f_L = \omega f_L^*$ with $f_L^* \in \text{span}\{U_l\}_{l=0}^L$. Thus, by continuity of the duality product

$$|\langle f - \omega f_L^* \,,\, g\rangle| \leq \left\|\omega^{1/2}(f - \omega f_L^*)\right\|_{L^2(\hat{\Gamma})} \left\|\omega^{-1/2} g\right\|_{L^2(\hat{\Gamma})}. \tag{2.22}$$

On one hand, it holds (Lions & Magenes, 1968; Grisvard, 1985)

$$\left\|\omega^{-1/2} g\right\|_{L^2(\hat{\Gamma})} \leq C \left\|g\right\|_{H^{1/2}(\hat{\Gamma})}, \tag{2.23}$$

while

$$\left\|\sqrt{\omega}(f - \omega f_L^*)\right\|_{L^2(\hat{\Gamma})} \leq \|f - \omega f_L^*\|_{L^2(\hat{\Gamma})}. \tag{2.24}$$

Set $\delta = \dfrac{\epsilon}{2C}$. By Lemma 1, there exists a $f_1^\delta \in L^\infty(\hat{\Gamma})$ such that

$$\|(f - \omega f_L^*)\|_{L^2(\hat{\Gamma})} \leq \left\|f - \omega f_1^\delta\right\|_{L^2(\hat{\Gamma})} + \left\|\omega(f_L^* - f_1^\delta)\right\|_{L^2(\hat{\Gamma})} \tag{2.25}$$

$$\leq \qquad \frac{\epsilon}{2C} \qquad + \left\|f_L^* - f_1^\delta\right\|_{L^2(\hat{\Gamma})}. \tag{2.26}$$

By density of continuous functions in $L^2(\hat{\Gamma})$ and again Weierstrass' theorem, there is a $L \in \mathbb{N}$ then such that

$$\left\|f_L^* - f_1^\delta\right\|_{L^2(\hat{\Gamma})} \leq \epsilon/2C, \tag{2.27}$$

from where

$$\|f - \omega f_L^*\|_{L^2(\hat{\Gamma})} \leq \frac{\epsilon}{C}. \tag{2.28}$$

By replacing the above in (2.24) and using (2.23), (2.22) becomes

$$|\langle f - f_L \,,\, g\rangle| = |\langle f - \omega f_L^* \,,\, g\rangle| \leq \epsilon \left\|g\right\|_{H^{1/2}(\hat{\Gamma})}, \tag{2.29}$$

from where (2.21) follows. □

Next, we use the family $\{\hat{\mathbb{T}}_L\}_{L\in\mathbb{N}}$ to define an approximation bases for the spaces $\mathbf{V}_i^{\text{pw}}$ of unknown Dirichlet and Neumman traces by using the mapping h_{ij} introduced in Section 2.3.1. Specifically, we define at each interface Γ_{ij}, the basis functions $\boldsymbol{\lambda}_m^{ij} := \hat{\boldsymbol{\lambda}}_m \circ h_{ij}^{-1}$,

$m \in \mathbb{N}_0$, such that, over each subdomain boundary $\partial\Omega_i$, we build functions:

$$\boldsymbol{\lambda}_m^i := \sum_{j\in\Lambda_i} \boldsymbol{\lambda}_m^{ij} \mathbf{1}_{\Gamma_{ij}}. \tag{2.30}$$

As expected, these functions are piecewise polynomials of degree L over $\partial\Omega_i$. Analogously, we use $\{\hat{\mathbb{Q}}_L\}_{L\in\mathbb{N}}$ to devise suitable test functions. First, set $\boldsymbol{\varphi}_l^{ij} := \hat{\boldsymbol{\varphi}}_l \circ h_{ij}^{-1}$, $l \in \mathbb{N}_0$, then

$$\boldsymbol{\varphi}_l^i := \sum_{j\in\Lambda_i} \boldsymbol{\varphi}_l^{ij} \mathbf{1}_{\Gamma_{ij}}. \tag{2.31}$$

Notice that the test functions satisfy

$$\boldsymbol{\varphi}_l^i(\mathbf{y}) = 0 \ , \ \forall\, \mathbf{y} \in \partial\Gamma_{ij}, \quad j \in \Lambda_i. \tag{2.32}$$

Although this property is required for functions conforming in $\widetilde{H}^{1/2}(\Gamma_{ij})$, it has a more practical use: it improves the computation of the discretized integral operators entries, as will be seen in section 2.3.3.

Provided with the above definitions, we are set to define the discrete spaces for trial and test functions over $\partial\Omega_i$ used to approximate solutions of (2.7):

$$\mathbf{V}_{i,N_i}^{\text{pw}} := \operatorname{span}\{\boldsymbol{\lambda}_m^i\}_{m=0}^{N_i} \qquad \text{and} \qquad \tilde{\tilde{\mathbf{V}}}_{i,N_i} := \operatorname{span}\{\boldsymbol{\varphi}_l^i\}_{l=0}^{N_i}. \tag{2.33}$$

For $\mathbf{N} = (N_0, N_1, N_2) \in \mathbb{N}^3$, we set cartesian product spaces

$$\mathbb{V}_{\mathbf{N}}^{\text{pw}} := \prod_{i=0}^{2} \mathbf{V}_{i,N_i}^{\text{pw}} \qquad \text{and} \qquad \tilde{\tilde{\mathbb{V}}}_{\mathbf{N}} := \prod_{i=0}^{2} \tilde{\tilde{\mathbf{V}}}_{i,N_i} \ . \tag{2.34}$$

PROPOSITION 2.2. *Let $N \in \mathbb{N}$, and $\mathbf{N} = (N, N, N) \in \mathbb{N}^3$, then $\{\mathbb{V}_{\mathbf{N}}^{pw}\}_{N\in\mathbb{N}}$ and $\{\tilde{\tilde{\mathbb{V}}}_{\mathbf{N}}\}_{N\in\mathbb{N}}$ are dense sequences of subspaces of $\mathbb{V}^{pw}$ and $\tilde{\tilde{\mathbb{V}}}$, respectively.*

PROOF. Follows directly from Proposition 2.1. □

2.3.3. BIOs approximation - Computational strategy

Armed with the above results, we now focus on the construction of the Galerkin-Petrov matrices originating from the MTF presented in Section 2.2.5. Particular attention is made to the approximation of the BI kernels and acceleration via FFT techniques (Trefethen, 2013; Bruno & Reitich, 2008). We need to compute integrals of the canonical form:

$$I_{\mathsf{L}}[m,l] = \left\langle \mathsf{L}\hat{\lambda}_m \, , \, \hat{q}_l \right\rangle = \int_{\hat{\Gamma}} \int_{\hat{\Gamma}} F_{\mathsf{L}}(s,t) T_m(s) \omega(t) U_l(t) ds dt, \tag{2.35}$$

where L is any of the BIOs and F_{L} represents the associated kernel including mappings required to push interfaces Γ_{ij} onto $\hat{\Gamma}$. The strategy followed relies on two steps:

(i) **Kernel approximation**. We first approximate the kernel F_{L} as a degenerate kernel using Chebyshev polynomials. Since Chebyshev polynomials can be directly be connected with Fourier series (Trefethen, 2013, Chap. 3), one can make use of the FFT to compute coefficients $g_n(t)$ such that

$$F(s,t) \approx \sum_{n=0}^{N_c} g_n(t) T_n(s), \tag{2.36}$$

for a suitable choice of N_c. Alternatively, using (2.12) the approximation (2.36) can be rewritten in terms of second kind Chebyshev polynomials as

$$F(s,t) \approx \sum_{n=0}^{N_c} f_n(t) U_n(s). \tag{2.37}$$

A discussion on these numerical kernel approximation is given in Section 2.4.1.

(ii) **Orthogonality**. By applying the orthogonality properties of Chebyshev polynomials, one can quickly obtain expressions of the form

$$I_{\mathsf{L}}[m,l] \approx \frac{\pi}{2} c_l \int_{-1}^{+1} f_m(t) T_m(t) dt \tag{2.38}$$

which can be computed by either the trapezoidal method or Gauss-Legendre quadrature.

Parallel to the above, one should be aware of the existence of two different singular behaviors in the integrands depending on whether the interfaces Γ_{ij} and Γ_{ik} coincide or not, i.e. for $j, k \in \Lambda_i$. Specifically,

- If $j \neq k$, the singularity occurs only at $s = t = \pm 1$, where the Chebyshev expansion loses accuracy.
- If $j = k$ singularities lie on the line $t = s$ with $t, s \in \hat{\Gamma}$. In this case, we follow standard regularization techniques (Hu, 1995; Farina, 2001) to extract the singularity.

2.3.3.1. Single layer operator (V_i) computation

The singular layer BIO maps Neumann trace data to Dirichlet one. Given the piecewise structure of our approximation bases, the discretization of the bilinear form associated to the single layer becomes, for $m, l \in \mathbb{N}_0$,

$$\begin{aligned} I_{\mathsf{V}_i}[l,m] := \left\langle \mathsf{V}_i \lambda^i_{\mathrm{N},l} \,,\, \varphi^i_{\mathrm{D},m} \right\rangle_{\partial\Omega_i} &= \left\langle \mathsf{V}_i \lambda^i_{\mathrm{N},l} \,,\, \sum_{j\in\Lambda_i} q^{ij}_m \mathbf{1}_{\Gamma_{ij}} \right\rangle_{\partial\Omega_i} \\ &= \sum_{j\in\Lambda_i} \left\langle \mathsf{V}_i \lambda^i_{\mathrm{N},l} \,,\, q^{ij}_m \right\rangle_{\Gamma_{ij}} \end{aligned} \tag{2.39}$$

At the same time,

$$\begin{aligned} \mathsf{V}_i \lambda^i_{\mathrm{N},l}(\mathbf{x}) &= \left\langle G_i(\mathbf{x},\cdot) \,,\, \sum_{k\in\Lambda_i} \lambda^{ik}_{\mathrm{N},l} \mathbf{1}_{\Gamma_{ik}} \right\rangle_{\partial\Omega_i} \\ &= \sum_{k\in\Lambda_i} \left\langle G_i(\mathbf{x},\cdot) \,,\, \lambda^{ik}_{\mathrm{N},l} \right\rangle_{\Gamma_{ik}} \end{aligned} \tag{2.40}$$

To be even more explicit, (2.39) reads,

$$I_{\mathsf{V}_i}[l,m] = \sum_{j\in\Lambda_i} \sum_{k\in\Lambda_i} \left\langle \left\langle G_i(\mathbf{x},\cdot) \,,\, \lambda^{ik}_{\mathrm{N},l} \right\rangle_{\Gamma_{ik}} \,,\, q^{ij}_m \right\rangle_{\Gamma_{ij}} \tag{2.41}$$

We study the summands $I^{jk}_{\mathsf{V}_i}[l,m] := \left\langle \left\langle G_i(\mathbf{x},\cdot)\,,\, \lambda^{ik}_{\mathrm{N},l} \right\rangle_{\Gamma_{ik}}\,,\, q^{ij}_m \right\rangle_{\Gamma_{ij}}$. By continuity, we can write

$$I^{jk}_{\mathsf{V}_i}[l,m] = \int_{\hat{\Gamma}}\int_{\hat{\Gamma}} G_i\left(\|h_{ij}(s)-h_{ik}(t)\|_2\right) U_l(t)\omega(s)U_m(s)\,\|h'_{ik}(t)\|\,\left\|h'_{ij}(s)\right\|\,dsdt \tag{2.42}$$

Case $j \neq k$. The term $G_i\left(\|h_{ij}(s)-h_{ik}(t)\|_2\right)$ presents at most two singularities corresponding to the end points, i.e. $t=s=\pm 1$. For all $t\in(-1,1)$, Weierstrass' theorem (Trefethen, 2013, Chap. 6) guarantees that the approximation by the Chebyshev expansion,

$$G_i\left(\|h_{ij}(s)-h_{ik}(t)\|_2\right)\left|h'_{ij}(s)\right| \approx \sum_{n=0}^{N_c} g_n(t)T_n(s), \quad N_c\in\mathbb{N}, \tag{2.43}$$

converges uniformly to the left hand side, where coefficients $g_n(t)$ are computed by the FFT algorithm. By (2.12), series (2.43) can be written in terms of second kind Chebyshev polynomials, with coefficients $f_n(t)$, and by orthogonality property (2.17), one eliminates one of the integrals in (2.42) to retrieve

$$I^{jk}_{\mathsf{V}_i}[l,m] \approx \int_{-1}^{1} \frac{\pi}{2} f_m(t)U_l(t)\,\|h'_{ik}(t)\|\,dt, \qquad \text{for } j\neq k. \tag{2.44}$$

This last integral is obtained via quadrature as mentioned before. Note that coefficients $f_m(t)$ are only required for interior points, i.e. $t\in(-1,1)$.

Case $j=k$. To avoid this difficulty, the kernel G_i is regularized. Let us recall the kernel corresponding to the Laplacian problem (null frequency, $\kappa_i=0$):

$$G_0(\|\mathbf{x}-\mathbf{y}\|_2) = -\frac{1}{2\pi}\log\|\mathbf{x}-\mathbf{y}\|_2\,. \tag{2.45}$$

By using a Taylor expansion together with the series representation for the Hankel function to represent G_i (Abramowitz, 1988, Formula 9.1.3), one can deduce that for a C^1-parametrization h_{ij} of the interface, the following kernel subtraction is a continuous function (Hiptmair, Jerez-Hanckes, & Urzúa-Torres, 2013, Sect. 2.6), i.e.

$$H_i(t,s) := G_i(\|h_{ij}(s) - h_{ij}(t)\|_2) - G_0(|s-t|) \in C^0(\hat{\Gamma} \times \hat{\Gamma}), \tag{2.46}$$

This property leads to the splitting $I_{\mathsf{V}_i}[l,m] = I^1_{\mathsf{V}_i}[l,m] + I^2_{\mathsf{V}_i}[l,m]$ with

$$I^1_{\mathsf{V}_i}[l,m] := \int_{\hat{\Gamma}}\int_{\hat{\Gamma}} H_i(t,s) U_l(t)\omega(s)U_m(s) \left\|h'_{ij}(s)\right\| \|h'_{ik}(t)\| \, dsdt, \tag{2.47}$$

$$I^2_{\mathsf{V}_i}[l,m] := \int_{\hat{\Gamma}}\int_{\hat{\Gamma}} G_0(|s-t|) U_l(t)\omega(s)U_m(s) \left\|h'_{ij}(s)\right\| \|h'_{ik}(t)\| \, dsdt. \tag{2.48}$$

The regularity property of $H_i(t,s)\left\|h'_{ij}(s)\right\|$ allows uniform convergence for a Chebysev expansion, and thus, the computation of $I^1_{\mathsf{V}_i}$ is given by quadrature formula as in (2.38).

To calculate $I^2_{\mathsf{V}_i}$, we recall that the kernel G_0 can be written as a series of Chebyshev polynomials (Logarithmic, Over, & Interval, 2012, Prop. 4.13):

$$G_0(|t-s|) = \frac{1}{2\pi}\log 2 + \sum_{n=1}^{\infty} \frac{1}{n\pi} T_n(t)T_n(s), \qquad s \neq t \in \hat{\Gamma}. \tag{2.49}$$

Thus, we can quickly derive the following expansion:

$$G_0(|s-t|)\left\|h'_{ij}(s)\right\| \approx \sum_{n=0}^{\infty} v_n(t)U_n(s), \tag{2.50}$$

with final computation of $I^2_{\mathsf{V}_i}$ again carried out using (2.38).

2.3.3.2. Double layer operators $(\mathsf{K}_i, \mathsf{K}_i')$ computation

We only consider the case of K_i as similar arguments hold for its adjoint. Discretization of bilinear forms for $m, l \in \mathbb{N}_0$ are

$$\begin{aligned} I_{\mathsf{K}_i}[l,m] &:= \left\langle \mathsf{K}_i \lambda^i_{\mathrm{D},l} \,,\, \varphi^i_{\mathrm{N},m} \right\rangle_{\partial\Omega_i} = \left\langle \mathsf{K}_i \lambda^i_{\mathrm{D},l} \,,\, \sum_{j\in\Lambda_i} q^{ij}_m \mathbf{1}_{\Gamma_{ij}} \right\rangle_{\partial\Omega_i} \\ &= \sum_{j\in\Lambda_i} \left\langle \mathsf{K}_i \lambda^i_{\mathrm{D},l} \,,\, q^{ij}_m \right\rangle_{\Gamma_{ij}} . \end{aligned} \tag{2.51}$$

Again, the operator action on $\lambda^i_{\mathrm{D},l}$ can be written as

$$\mathsf{K}_i \lambda^i_{\mathrm{D},l}(\mathbf{x}) = \left\langle \frac{\partial G_i}{\partial n_{\mathbf{y}}}(\mathbf{x},\cdot) \,,\, \sum_{k\in\Lambda_i} \lambda^{ik}_{\mathrm{D},l} \mathbf{1}_{\Gamma_{ik}} \right\rangle_{\partial\Omega_i} = \sum_{k\in\Lambda_i} \left\langle \frac{\partial G_i}{\partial n_{\mathbf{y}}}(\mathbf{x},\cdot) \,,\, \lambda^{ik}_{\mathrm{D},l} \right\rangle_{\Gamma_{ik}}, \tag{2.52}$$

where the normal derivative of the Green kernel is

$$\frac{\partial G_i}{\partial n_{\mathbf{y}}} = -\kappa_i H_1^{(1)}(\kappa_i \left\|\mathbf{x}-\mathbf{y}\right\|_2) \frac{(\mathbf{y}-\mathbf{x})\cdot \mathbf{n}_y}{\left\|\mathbf{x}-\mathbf{y}\right\|_2}, \tag{2.53}$$

with $\mathbf{n}_y$ being the outward normal vector to the interface at the point y.

Case $j \neq k$. For double layer operators, singularities at $t = s = \pm 1$ are stronger than for the single layer case, i.e. compare $H_1^{(1)}(\kappa_i \left\|x-y\right\|_2) \sim \frac{1}{\left\|x-y\right\|_2}$ to $H_0^{(1)}(\kappa_i \left\|x-y\right\|_2) \sim \log \left\|x-y\right\|_2$, and thus, the approximation by Chebyshev polynomials is much worse when approaching the corners. Luckily, thanks to the weighted test function this singularities are smoothened yielding a precise approximation of I_{K_i} and $I_{\mathsf{K}_i'}$ (see Table 2.1).

Case $j = k$. To be able to apply to Chebyshev expansion, the kernel requires to be continuous, which is shown in the following proposition:

PROPOSITION 2.3 (Lemma 2.2.14 in (Sauter & Christoph, 2010)). *Let* $\mathbf{n}$ *denote the exterior normal to* Ω_i*. If* $\mathbf{n}$ *is continuous over* Γ_{ij}*, then there exists a bounded constant*

$c_{\mathbf{n}} > 0$ *such that*

$$|(\mathbf{y}-\mathbf{x})\cdot\mathbf{n}_y| \leq c_{\mathbf{n}} \|\mathbf{y}-\mathbf{x}\|_2^2, \qquad \mathbf{x}\neq\mathbf{y}\in\Gamma_{ij}. \tag{2.54}$$

Thus, it is straightfoward to show that if the interface Γ_{ij} is a C^1-curve then the double layer BIO kernel is continuous, and can be approximated by,

$$\frac{\partial G_i}{\partial n_{\mathbf{y}}}\left|h'_{ij}(s)\right| \approx \sum_{n=0}^{Nc} k_n(t)U_n(s) \tag{2.55}$$

and we can proceed as sketched at the beginning of Section 2.3.3.

2.3.3.3. Hypersingular operator (W_i) computation

Here we carry out the same piecewise summation over interfaces Γ_{ij} and recast the problem in terms of single layer operator as follows. First, recall that for a curve Γ piecewise smooth in $\mathbb{R}^2$ with unitary normal vector $\mathbf{n}$, and a $C^1(I)$-function defined on a neighborhood I of Γ, $f: I\to\mathbb{R}$, the curl operator reads

$$\operatorname{curl} f(\mathbf{x}) := n^1(\mathbf{x})\partial_2 f(\mathbf{x}) - n^2(\mathbf{x})\partial_1 f(\mathbf{x}) \quad , \quad \mathbf{x}\in\Gamma. \tag{2.56}$$

We then invoke the following result:

PROPOSITION 2.4 (Theorem 6.15 in (Steinbach, 2008)). *Let Γ be a sufficiently smooth, bounded curve in $\mathbb{R}^2$ and let g, f be $C^1(\Gamma)$ functions such that $g(\mathbf{y})=0$ for all $\mathbf{y}\in\partial\Gamma$. Then it holds*

$$\begin{aligned}\langle \mathsf{W}_i f\ ,\ g\rangle_{\partial\Omega_i} = \langle \mathsf{V}_i \operatorname{curl} f\ ,\ \operatorname{curl} g\rangle_{\partial\Omega_i} - \kappa_i^2 \langle \mathbf{n}_{\mathbf{x}}\cdot\mathbf{n}_{\mathbf{y}}\mathsf{V}_i f\ ,\ g\rangle_{\partial\Omega_i} \\ - f\int_\Gamma G_i(\|\mathbf{x}-\mathbf{y}\|)\operatorname{curl} g(\mathbf{y})d\Gamma_{\mathbf{y}})\Big|_{\mathbf{x}\in\partial\Gamma}.\end{aligned} \tag{2.57}$$

Thus, for $I_{\mathsf{W}_i}[l,m]$ we can also obtain a Fourier-Chebyshev series expansion. We establish explicit formulas for $\operatorname{curl}\hat{\lambda}_{\mathrm{D},m}$ and $\operatorname{curl}\hat{q}_l$ via the polynomial properties presented

in Section 2.3.2:

$$\operatorname{curl} \hat{\lambda}_{\mathrm{D},m} = T'_m = mU_{m-1}, \tag{2.58}$$

$$\operatorname{curl} \hat{q}_l = (\omega U_l)' = -\omega^{-1} T_{l+1}. \tag{2.59}$$

Since now test functions are expressed in terms of first kind Chebyshev polynomials, orthogonality relation (2.16) allows direct use of the Chebyshev expansion of the kernel. Note that the term,

$$\hat{\lambda}_{\mathrm{D},m} \int_{\Gamma_{ij}} G_i \operatorname{curl} \hat{q}_l d\Gamma \Big|_{x \in \partial\Gamma_{ij}} \tag{2.60}$$

is not accurate close to the corners ($t = \pm 1$) when $j \neq k$. To circumvent this issue, we observe that a corner belongs to two interfaces and, instead of considering the point on the interface Γ_{ij}, we take it on Γ_{ik}. This leads back to the case $j = i$ and kernel regularization is used to compute the required coefficient.

2.4. Numerical Results

We now present numerical simulations for a two-dimensional scatterer. We first examine the range of validity of our numerical approximations for the BIOs, then consider error convergence for fixed wavenumbers and with respect to a frequency sweep. Finally, we study the effect of preconditioning for iterative solvers.

The geometry considered is illustrated in Figure 2.2, and it consists of three domains: $\Omega_0 := \{\mathbf{x} \in \mathbb{R}^2, \|\mathbf{x}\|_2 > 1\}$, $\Omega_1 := \{\mathbf{x} \in \mathbb{R}^2, \|\mathbf{x}\|_2 < 1, x_1 < 0\}$, and $\Omega_2 := \{\mathbf{x} \in \mathbb{R}^2, \|\mathbf{x}\|_2 < 1, x_1 > 0\}$. This simple case contains all the difficulties portraying Lipschitz domains with sharp corners. The experiments were performed on MATLAB 2009b, 64-bit, running on a GNU/Linux desktop machine with 3.40GHz CPU and 32GB RAM. The discretization of the operators is computed by a MEX-C library. CPU times to compute the MTF system of moderate to high frequency (κ from 10 to 100) range between a few seconds to less than one hour.

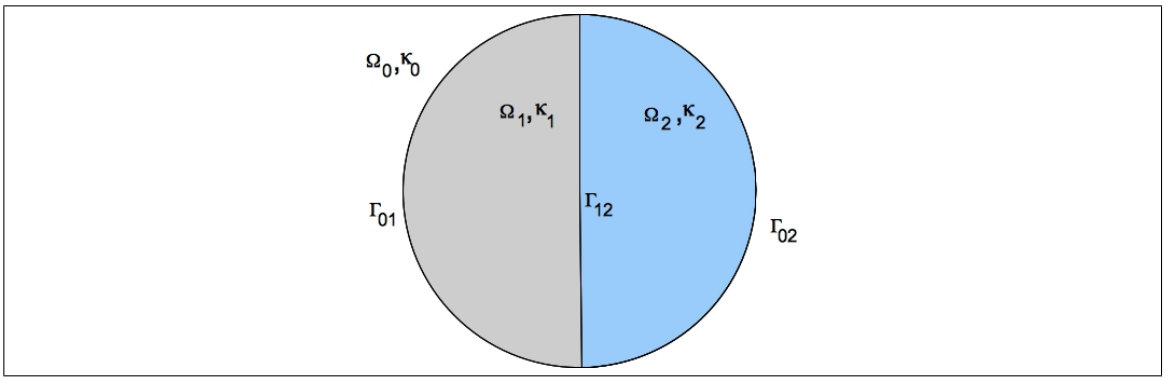

Figure 2.2. Canonical geometry used to test the spectral MTF method

Heuristically, the parameter used in the degenerate expansion of the kernels is given by $N_c = 2\text{ceil}(3N + \max \kappa_i) + 128$. Also observe that when considering N for the number of degrees of freedom, $2N + 1$ trial and test functions are considered .

2.4.1. BIOs numerical approximation

Let us define the following errors for different values of $N_c \in \mathbb{N}$ for a given $t \in \hat{\Gamma}$ and interface Γ_{ik}

$$e^{\mathsf{V}}_{\text{Cheb}}(t) := \left\| G_k(\|\mathbf{x}(t) - \mathbf{y}(s)\|)\, |(h'_{ik}(s)| - \sum_{n=0}^{N_c} g_n(t) T_n(s) \right\|_{L^2(\hat{\Gamma})},$$

$$e^{\mathsf{K}}_{\text{Cheb}}(t) := \left\| \frac{\partial G_i}{\partial n}(\|\mathbf{x}(t) - \mathbf{y}(s)\|)\, |h'_{ik}(s)| - \sum_{n=0}^{N_c} g_n(t) T_n(s) \right\|_{L^2(\hat{\Gamma})}$$

The errors of the discretized Galerkin-Petrov operators for entries $I_{\mathsf{L}}[m, l]$ are found by integrating over the next interface Γ_{ij}, and we drop the superscript ij in (2.42):

$$e_{I_{\mathsf{V}}}[m, l] := \left| I^{\text{Cheb}}_{\mathsf{V}}[m, l] - I^{\text{quad}}_{\mathsf{V}}[m, l] \right|,$$

$$e_{I_{\mathsf{K}}}(m, l) := \left| I^{\text{Cheb}}_{\mathsf{K}}[m, l] - I^{\text{quad}}_{\mathsf{K}}(m, l] \right|$$

where $I_{\mathsf{V}}^{\text{Cheb}}$, $I_{\mathsf{K}}^{\text{Cheb}}$ are the approximations of I_{V} and I_{K} using the method described on Sections 2.3.3.1 and 2.3.3.2, respectively. Values $I_{\mathsf{V}}^{\text{quad}}$, $I_{\mathsf{K}}^{\text{quad}}$ are approximations obtained using an expensive adaptative quadrature scheme. Results for a few cases are given in Table 2.1. The good accuracy of the approximation for $I_{\mathsf{V}}^{\text{Cheb}}$, $I_{\mathsf{K}}^{\text{Cheb}}$ arises from the smoothening behavior of the weighted test functions.

(a) $N_c = 128$

t	e^V_{Cheb}	$e_{I_V}(0,0)$	e^K_{Cheb}	$e_{I_K}(0,0)$
0.9	10^{-15}	10^{-14}	10^{-15}	10^{-12}
0.99	10^{-7}		10^{-8}	
0.9999	10^{-3}		10^{-3}	
$1-10^{-6}$	10^{-2}		10^{-1}	
$1-10^{-8}$	10^{-2}		10^{0}	

(b) $N_c = 1280$

t	e^V_{Cheb}	$e_{I_V}(0,0)$	e^K_{Cheb}	$e_{I_K}(0,0)$
0.9	10^{-15}	10^{-14}	10^{-15}	10^{-12}
0.99	10^{-14}		10^{-14}	
0.9999	10^{-8}		10^{-7}	
$1-10^{-6}$	10^{-4}		10^{-1}	
$1-10^{-8}$	10^{-2}		10^{0}	

(c) $N_c = 12800$

t	e^V_{Cheb}	$e_{I_V}(0,0)$	$e^K_{\text{Chebyshev}}$	$e_{I_K}(0,0)$
0.9	10^{-15}	10^{-14}	10^{-15}	10^{-12}
0.99	10^{-14}		10^{-14}	
0.9999	10^{-11}		10^{-11}	
$1-10^{-6}$	10^{-9}		10^{-6}	
$1-10^{-8}$	10^{-6}		10^{0}	

Table 2.1. Kernel approximation performances for different values of N_c.

2.4.2. Symmetric configuration

We study the case of one penetrable obstacle as described in Figure 2.2 with equal interior wavenumbers $\kappa_1 = \kappa_2$, and varying exterior wavenumber κ_0. Under these conditions, the exact solution is provided by means of Mie series (Warnick, 2008, Section 3.1.5) which is used to validate the model.

Figure 2.3 depicts convergence rates in different norms pointing out at a maximum number of degrees of freedom after which, no further convergence is achieved. This is due to the numerical approximation of the BIOs and is bounded by machine precision in the best case. In fact, the total number of trial and test functions required to reach a given accuracy can be derived from asymptotics of the underlying Mie series. From these figures, one can observe that this number is not completely linear with the wavenumber, e.g., for an error of 10^{-4}, $N \approx 12$ at $\kappa_0 = 10$, $N \approx 45$ at $\kappa_0 = 50$ and $N \approx 80$ at $\kappa_0 = 100$. More details about the number of degrees of freedom is given in Section 2.4.4. On the other hand, the error derived from the weak Calderón identities on Figure 2.6 are defined as the Euclidean norm of the vector $v = \langle 2A_i\lambda^i, \phi^i\rangle - \langle \lambda^i, \phi^i\rangle$.

2.4.3. Asymmetric configuration

Subdomains Ω_1 and Ω_2 portrayed in Figure 2.2 are now given different wavenumbers, $\kappa_1 = 50$ and $\kappa_2 = 1$, with exterior wavenumber set to $\kappa_0 = 100$. In this configuration, solutions cannot be computed via Mie series nor is there any analytic solution available. To validate the model, we check whether jump relations (2.3b) and (2.3c) are fulfilled.

Figures 2.4 and 2.5 show traces defined on each interface for the mentioned case. Expected jump relations (2.3c) and (2.3b) are satisfied and their corresponding error is of magnitude 10^{-12} in L^2-norm. Note that the Neumann traces are not continuous at the triple points, e.g., at angles $-90°$, $90°$, $270°$, which are taken into account by the discontinuous trial functions belonging to $\mathbf{V}_0^{\text{pw}}$.

2.4.4. Error convergence frequency analysis

Until now we have only verified that the model works for different wavenumbers. However, for most applied models, one usually fixes physical parameters and seeks for solutions over a frequency range. To illustrate this, we recall the wavenumber definition for the electromagnetic case per subdomain, $\kappa_i = \omega_0\sqrt{\epsilon_i\mu_i}$, where ϵ_i and μ_i are the dielectric and permeability constants, respectively, and ω_0 is the radial frequency of excitation.

To simplify our analysis, we set permeabilities $\mu_i = 1$, for all $i = 0, 1, 2$, and set $\epsilon_0 = 1$ so that wavenumbers become $\kappa_0 = \omega_0$, $\kappa_i = \kappa_0\sqrt{\epsilon_i}$, $i \in \{1, 2\}$. We now fix ϵ_i and compute the error for a range of values of κ_0 . For every κ_0, we need to determine the number of test and trial functions. Based on some ideas of the truncation of the Mie series (Warnick, 2008), for the symmetric case we tried three different rules, with their specifications given in Figure 2.6.

We observe that for the symmetric case the three rules have a similar behavior so we choose the rule minimizing the number of degrees of freedom, $2N_i + 1 = 1.1\kappa_i + 7$. We repeat the same experiment but now for an asymmetric arrangement, $\epsilon_1 = 2, \epsilon_2 = 3$, for which results are displayed in Figure 2.7. As can be seen, only the rule $2N_i + 1 = 1.1\max_i\{\kappa_i\} + 7$ works for all the cases but is not optimal in terms of degrees of freedom. The reason behind this lack of clear knowledge stems from the lack of Mie series and deserves future investigation.

2.4.5. Performance using iterative solvers - Preconditioning

When the wavenumber increases, the Helmholtz equation becomes more indefinite, hence, the convergence rate of iterative solvers based on Krylov subspace, e.g. *Generalized Minimal Residual* (GMRes)method, is either poor or not achieved (Saad, 2002, Chapter 6). To tackle this, one traditionally resorts to different preconditioning schemes (Ernst & Gander, 2011; Erlangga, 2008; Benzi, 2002).

The Calderón identity, used to establish MTF, leads to a built-in preconditioner given by the block diagonal operator,

$$\mathbf{A} := \begin{pmatrix} \mathsf{A}_0 & 0 & 0 \\ 0 & \mathsf{A}_1 & 0 \\ 0 & 0 & \mathsf{A}_2 \end{pmatrix}, \tag{2.61}$$

whose discrete form is already computed. More precisely, the discrete Calderón identity becomes a mass-like matrix M_{ass} with a block diagonal composed by duality products. The duality pairings for the Neumann trace yield a identity-like matrix due to the orthogonality of first kind Chebyshev polynomials, while for Dirichlet traces one obtains a bi-diagonal matrix coming from recursion and orthogonality properties between first and second kind Chebyshev polynomials.

The preconditioning matrix explicitly reads,

$$\mathsf{P} = \mathsf{M}_{ass}^{-1}\mathbf{A} \tag{2.62}$$

where $\mathbf{A}$ the discretization of (2.61) and M_{ass}^{-1} is the mass-like matrix. Since the structure of the mass matrix is diagonal per block, the numerical cost of its inverted matrix-vector product is negligible compared to the dense matrix-vector product originated by $\mathbf{A}$. We use the naive strategy to carry out a LU-factorization of the relative small bi-diagonal blocks, which means a simple reordering, and then perform sparse substitutions at each iteration of GMres method.

Note that the discretization form used in (2.61) to build the preconditioner is not necessarily the optimal one to tackle the wavenumber dependency (Hiptmair, 2006; Steinbach & Wendland, 1998). However, the proposed preconditioner requires a negligible numerical cost.

Figure 2.8 shows the convergence history for a homogeneous case ($\kappa_1 = \kappa_2 = 1$) and a heterogeneous case ($\kappa_1 = 50$, $\kappa_2 = 1$), both comparing GMRes (Saad & Schultz, 1986)

without and with the block diagonal preconditioner proposed P, at moderate frequency ($\kappa_0 = 10$) and high frequency ($\kappa_0 = 100$). One can observe the significant reduction in number of iterations for the preconditioned system, while the convergence of the unpreconditioned system becomes unacceptable. In terms of CPU time, the solution by GMRes without preconditioner (resp. with), including preprocessing of factorization, requires 18s (resp. 2s) for the case $\kappa_0 = 10$, $\kappa_1 = 50$, $\kappa_2 = 1$, and 245s (resp. 30s) for the case $\kappa_0 = 100,\ \kappa_1 = 50 \mid 1,\ \kappa_2 = 1$.

2.5. Conclusions and Future Work

We have presented a robust and efficient method that allows the modeling of scattering by heterogeneous penetrable scatters for large frequency ranges. Robustness is due to the lack of spurious modes and large frequency sweep that can be practically handled. Efficiency comes from two sources: the parallelizable character of the formulation along with the choice of discretization bases. Computation of matrix entries resulting from the Galerkin-Petrov discretization proposed can be quickly computed using FFT and regularization techniques. Moreover, the method yields a built-in preconditioner, as its diagonal and mass matrix can be reused to improve convergence of iterative solvers as GMRes, just as previously shown for low-order elements. Nonetheless, although a rule of thumb has been given to obtain the number of Chebyshev polynomials required, better estimates should be sought after. Also, particular attention should be given to integration routines for boundary integral operator.

Future research directions focus on a more detailed study of related preconditioning schemes: their dependency on wavenumbers, contrast and the relation to operator preconditioning. Also we intend to continue improving code efficiency by accelerating matrix-vectors computations by compression and its extension three-dimensions.

Acknowledgement

We thank Prof. Oscar Bruno for his valuable comments over a discussion concerning a draft of the present work.

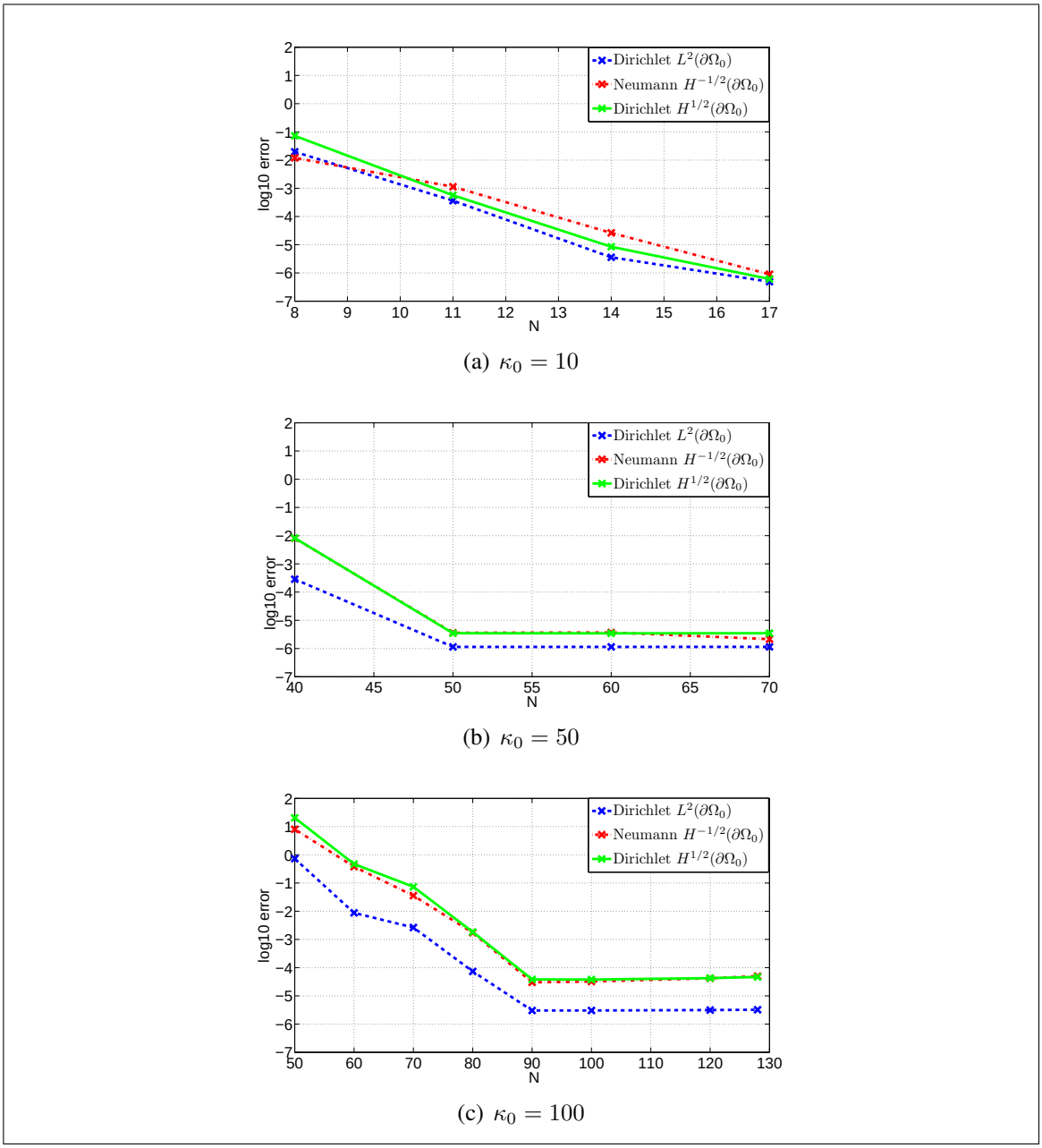

(a) $\kappa_0 = 10$

(b) $\kappa_0 = 50$

(c) $\kappa_0 = 100$

Figure 2.3. Error convergence for the exterior trace in different norms for the Dirichlet and Neumann traces $(\lambda_0^{\mathrm{D}}, \lambda_0^{\mathrm{N}})$ on $\partial\Omega_0$ for two half-circles with $\kappa_1 = \kappa_2 = 1$ and different values of κ_0. The impinging plane wave comes at an angle $\theta = 0^\circ$ but similar behaviors are obtained for other angles. Exact traces are obtained via Mie series.

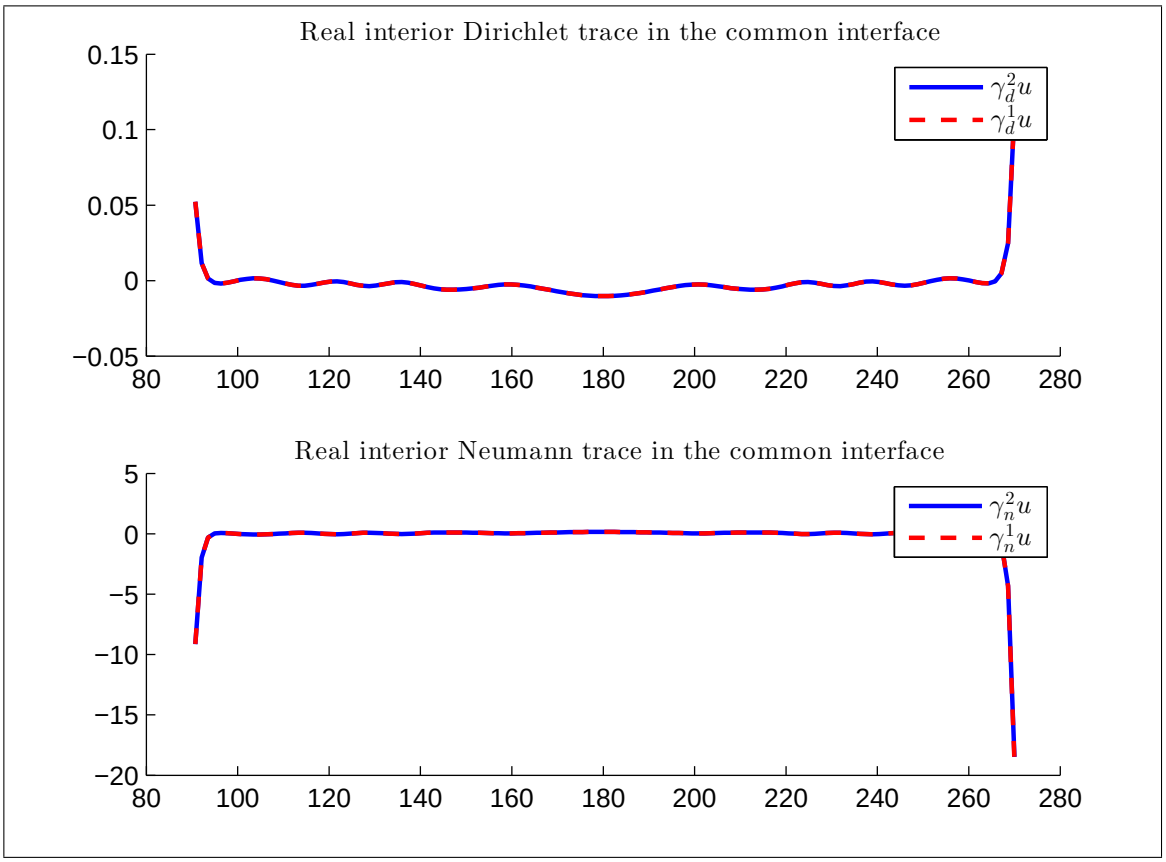

Figure 2.4. Dirichlet and Neumann traces $(\lambda_{1,2}^{\mathrm{D}}, \lambda_{1,2}^{\mathrm{N}})$ in the common interface Γ_{12}, one taken from Ω_1 (dashed-red), and another one taken from Ω_2 (blue). The values of the wavenumber are $\kappa_0 = 100$, $\kappa_1 = 50$ and $\kappa_2 = 1$ for an impinging plane wave at an angle $\theta = 0°$. The x-axis represents the coordinate parametrization and the y-axis represents the real part of the traces in arbitrary units.

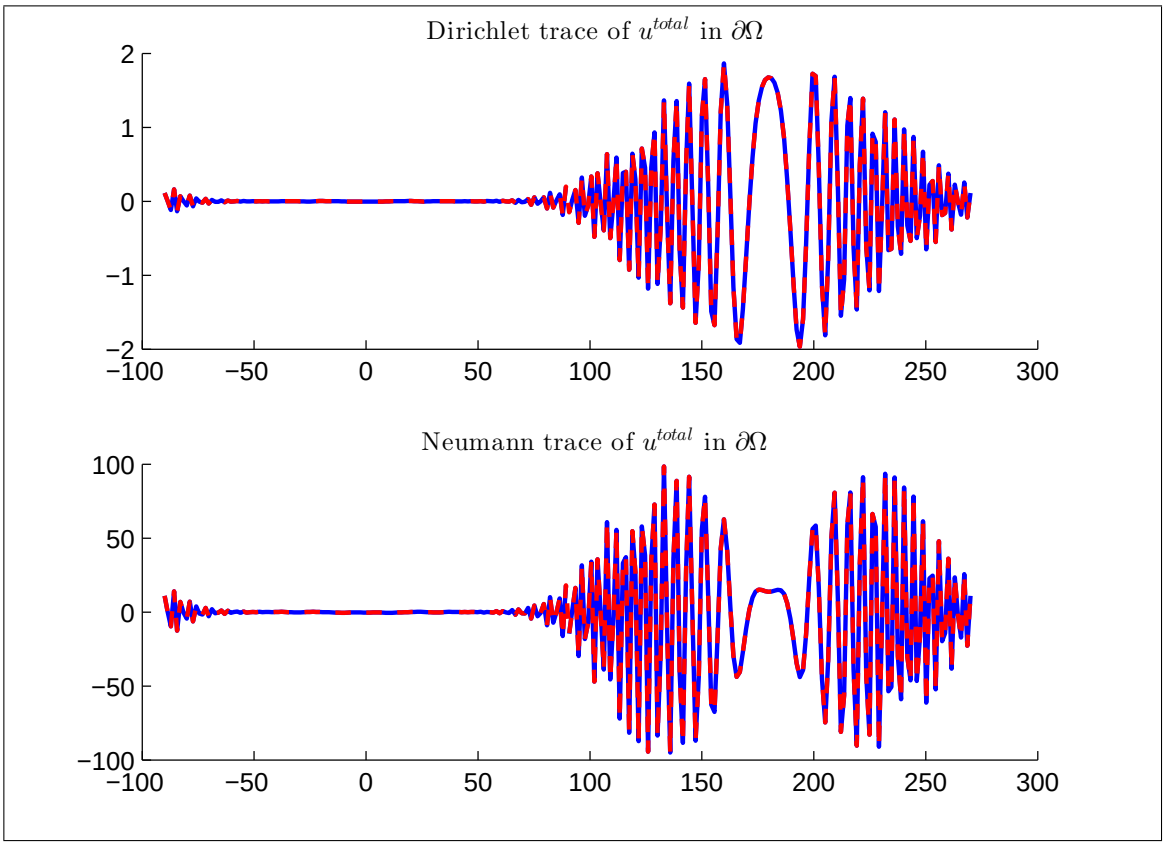

Figure 2.5. Dirichlet and Neumann traces at interfaces Γ_{01} and Γ_{02}, one with the incident field included taken from outside (Ω_0) in dashed-red, and another one taken from inside $\Omega_{1,2}$ in blue. Wavenumber values are $\kappa_0 = 100$, $\kappa_1 = 50$ and $\kappa_2 = 1$, for an impinging plane wave with angle $\theta = 0$. The x-axis represents the coordinate parametrization and the y-axis represents the real part of the traces in arbitrary unit.

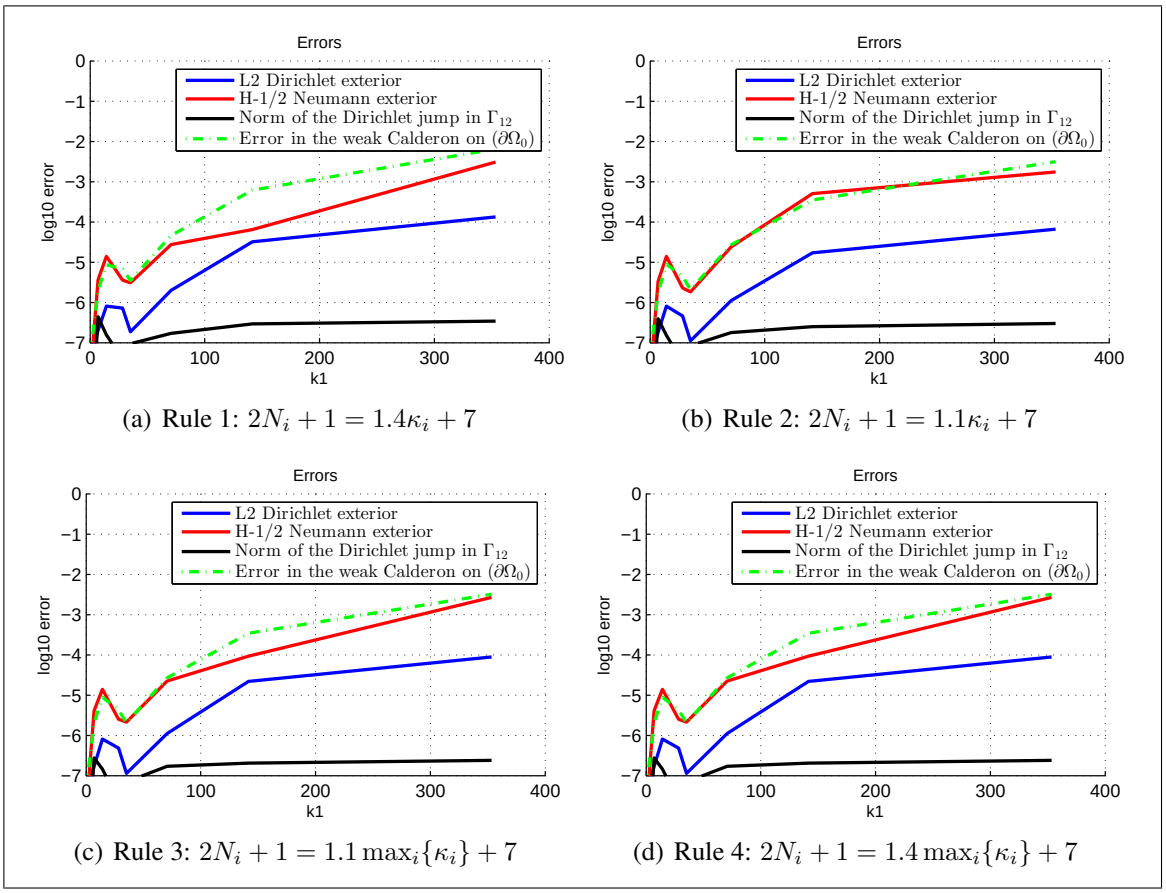

(a) Rule 1: $2N_i + 1 = 1.4\kappa_i + 7$

(b) Rule 2: $2N_i + 1 = 1.1\kappa_i + 7$

(c) Rule 3: $2N_i + 1 = 1.1 \max_i\{\kappa_i\} + 7$

(d) Rule 4: $2N_i + 1 = 1.4 \max_i\{\kappa_i\} + 7$

Figure 2.6. Error performance versus wavenumber $\kappa_0 \in [0, 250]$ in different norms for the symmetric case .

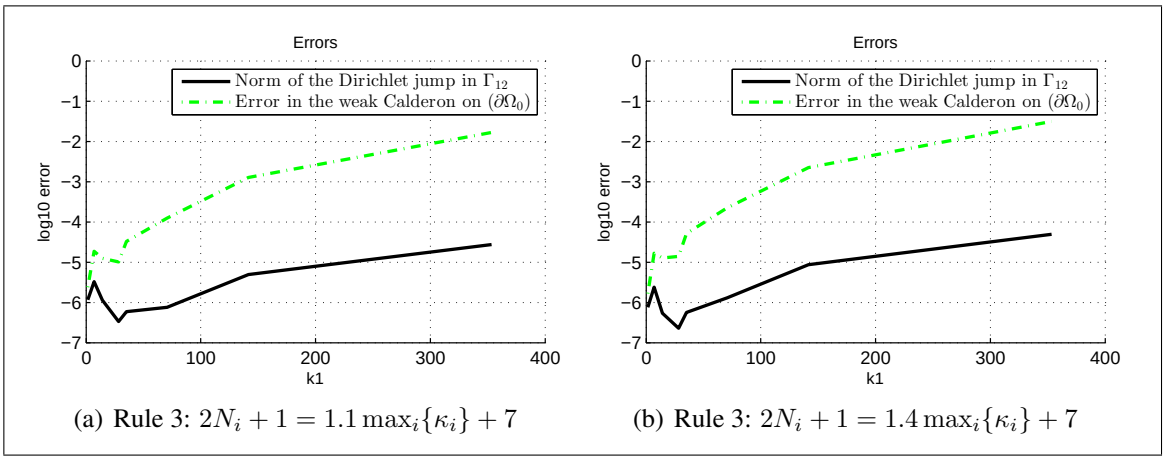

(a) Rule 3: $2N_i + 1 = 1.1 \max_i\{\kappa_i\} + 7$

(b) Rule 3: $2N_i + 1 = 1.4 \max_i\{\kappa_i\} + 7$

Figure 2.7. Errors in different norms for increasing frequencies, $\kappa_0 \in [0, 250]$ asymmetric case.

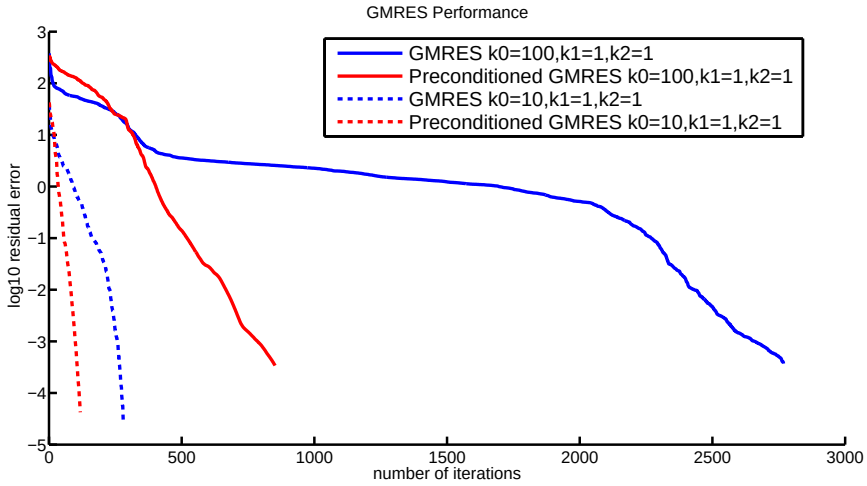

(c) Symmetric case: $\kappa_1 = \kappa_2 = 1$, Size: 420 ($\kappa_0 = 10$) and 3084 ($\kappa_0 = 100$)

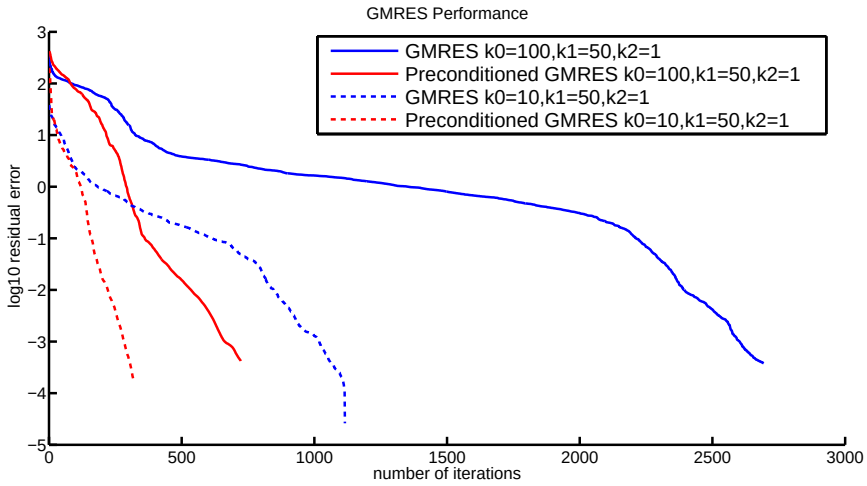

(d) Asymmetric case: $\kappa_1 = 50$, $\kappa_2 = 1$, Size: 1232 ($\kappa_0 = 10$) and 3084 ($\kappa_0 = 100$)

Figure 2.8. Residual error in two-norm against number of iterations for GMRes (no restart). The preconditioner is applied on the left side of the linear system.

REFERENCES

Abramowitz, M. (1988). *Handbook of Mathematical Functions with Formulas, Graphs, and Mathematical Tables* (Vol. 56). doi: 10.1119/1.15378

Ammari, H. (2008). *An Introduction to mathematics of emerging biomedical imaging*. Berlin, London: Springer. Retrieved from http://opac.inria.fr/record=b1125776

Anand, A., Boubendir, Y., Ecevit, F., & Reitich, F. (2010). Analysis of multiple scattering iterations for high-frequency scattering problems. II. The three-dimensional scalar case. *Numer. Math.*, *114*(3), 373–427. Retrieved from http://dx.doi.org/10.1007/s00211-009-0263-1 doi: 10.1007/s00211-009-0263-1

Bebendorf, M. (2008). *Hierarchical Matrices: A Means to Efficiently Solve Elliptic Boundary Value Problems*. Springer. Retrieved from http://books.google.ca/books?id=hnIJOwyz9Z4C

Benzi, M. (2002). Preconditioning techniques for large linear systems: A survey. *Journal of Computational Physics*, *182*, 418–477. doi: doi:10.1006/jcph.2002.7176

Borden, B. (1999). *Radar Imaging of Airborne Targets: A Primer for Applied Mathematicians and Physicists*. Taylor & Francis. Retrieved from http://books.google.cl/books?id=R-EQzoT34W4C

Bruno, O. P., & Lintner, S. K. (2013). A high-order integral solver for scalar problems of diffraction by screens and apertures in three-dimensional space. *J. Comput. Phys.*, *252*, 250–274. Retrieved from http://dx.doi.org/10.1016/j.jcp.2013.06.022 doi: 10.1016/j.jcp.2013.06.022

Bruno, O. P., & Reitich, F. (2008). High-order methods for high-frequency scattering applications. In *Modeling and computations in electromagnetics* (Vol. 59, pp. 129–163). Springer, Berlin. Retrieved from http://dx.doi.org/10.1007/

978-3-540-73778-0_5 doi: 10.1007/978-3-540-73778-0_5

Chandler-Wilde, S. N., Graham, I. G., Langdon, S., & Spence, E. A. (2012). Numerical-asymptotic boundary integral methods in high-frequency acoustic scattering. *Acta Numer.*, *21*, 89–305.

Chen, J. T., & Chiu, Y. P. (2002). On the pseudo-differential operators in the dual boundary integral equations using degenerate kernels and circulants. *Engineering Analysis with Boundary Elements*, *26*(1), 41-53.

Claeys, X., & Hiptmair, R. (2013). Multi-trace boundary integral formulation for acoustic scattering by composite structures. *Comm. Pure Appl. Math.*, *66*(8), 1163–1201. Retrieved from http://dx.doi.org/10.1002/cpa.21462 doi: 10.1002/cpa.21462

Claeys, X., Hiptmair, R., & Jerez-Hanckes, C. (2013). Multitrace boundary integral equations. In *Direct and inverse problems in wave propagation and applications* (Vol. 14, pp. 51–100). De Gruyter, Berlin.

Claeys, X., Hiptmair, R., Jerez-Hanckes, C., & Pintarelli, S. (2014, February). *Novel multi-trace boundary integral equations for transmission boundary value problems* (Tech. Rep. No. 2014-5). Seminar for Applied Mathematics, ETH Zurich.

Darrigrand, E. (2002). Coupling of fast multipole method and microlocal discretization for the 3-D Helmholtz equation. *J. Comput. Phys.*, *181*(1), 126–154. Retrieved from http://dx.doi.org/10.1006/jcph.2002.7091 doi: 10.1006/jcph.2002.7091

Darve, E., & Havé, P. (2004a). Efficient fast multipole method for low-frequency scattering. *J. Comput. Phys.*, *197*(1), 341–363. Retrieved from http://dx.doi.org/10.1016/j.jcp.2003.12.002 doi: 10.1016/j.jcp.2003.12.002

Darve, E., & Havé, P. (2004b). A fast multipole method for Maxwell equations stable at all frequencies. *Philos. Trans. R. Soc. Lond. Ser. A Math. Phys. Eng. Sci.*, *362*(1816), 603–628. Retrieved from http://dx.doi.org/10.1098/rsta.2003.1337 doi: 10.1098/rsta.2003.1337

de La Bourdonnaye, A. (1994). High frequency approximation of integral equations modeling scattering phenomena. *RAIRO Modél. Math. Anal. Numér.*, *28*(2), 223–241.

Domínguez, V., Graham, I. G., & Smyshlyaev, V. P. (2007). A hybrid numerical-asymptotic boundary integral method for high-frequency acoustic scattering. *Numer. Math.*, *106*(3), 471–510. Retrieved from http://dx.doi.org/10.1007/s00211-007-0071-4 doi: 10.1007/s00211-007-0071-4

Ecevit, F., & Reitich, F. (2009). Analysis of multiple scattering iterations for high-frequency scattering problems. I. The two-dimensional case. *Numer. Math.*, *114*(2), 271–354. Retrieved from http://dx.doi.org/10.1007/s00211-009-0249-z doi: 10.1007/s00211-009-0249-z

Erlangga, Y. (2008). Advances in iterative methods and preconditioners for the helmholtz equation. *Archives of Computational Methods in Engineering*, *15*, 37-66. Retrieved from http://dx.doi.org/10.1007/s11831-007-9013-7 (10.1007/s11831-007-9013-7)

Ernst, O., & Gander, M. (2011). Why it is difficult to solve helmholtz problems with classical iterative methods. *Numerical Analysis of Multiscale Problems*.

Farina, L. (2001, January). Evaluation of Single Layer Potentials over Curved Surfaces. *SIAM Journal on Scientific Computing*, *23*(1), 81–91. Retrieved from http://epubs.siam.org/doi/abs/10.1137/S1064827599363393 doi: 10.1137/S1064827599363393

Grisvard, P. (1985). *Elliptic problems in nonsmooth domains* (Vol. 24). Pitman (Advanced Publishing Program), Boston, MA.

Hewett, D. P., Langdon, S., & Melenk, J. M. (2013). A high frequency hp boundary element method for scattering by convex polygons. *SIAM J. Numer. Anal.*, *51*(1), 629–653. Retrieved from http://dx.doi.org/10.1137/110856812 doi: 10.1137/110856812

Hiptmair, R. (2006). Operator preconditioning. *Computers & Mathematics with*

Applications, *52*(5), 699 - 706. Retrieved from http://www.sciencedirect.com/science/article/pii/S0898122106002495 doi: http://dx.doi.org/10.1016/j.camwa.2006.10.008

Hiptmair, R., & Jerez-Hanckes, C. (2012, October). Multiple traces boundary integral formulation for Helmholtz transmission problems. *Advances in Computational Mathematics*, *37*(1), 39–91. Retrieved from http://link.springer.com/10.1007/s10444-011-9194-3 doi: 10.1007/s10444-011-9194-3

Hiptmair, R., Jerez-Hanckes, C., & Urzúa-Torres, C. (2013). *Optimal operator preconditioning for boundary elements on open curves* (Tech. Rep. No. 2013-48). ETH Zurich.

Hu, F. Q. (1995). A spectral boundary integral equation method for the 2-D Helmholtz equation. *Computational Physics*, *120*(2), 340–347.

Jerez-Hanckes, C., & Nédélec, J.-C. (2012). Explicit variational forms for the inverses of integral logarithmic operators over an interval. *SIAM J. Math. Anal.*, *44*(4), 2666–2694. Retrieved from http://dx.doi.org/10.1137/100806771 doi: 10.1137/100806771

Jin, J. M. (2011). *Theory and Computation of Electromagnetic Fields*. Wiley. Retrieved from http://books.google.cl/books?id=D6SqmxJVV5wC

Lin, P. D. (2014). *New computation methods for geometrical optics* (Vol. 178). Springer, Singapore. Retrieved from http://dx.doi.org/10.1007/978-981-4451-79-6 doi: 10.1007/978-981-4451-79-6

Lions, J.-L., & Magenes, E. (1968). *Problèmes aux limites non homogènes et applications. Vol. 1*. Dunod, Paris.

Logarithmic, I., Over, O., & Interval, A. N. (2012). Downloaded 08 / 06 / 14 to 146 . 155 . 157 . 11 . Redistribution subject to SIAM license or copyright ; see http://www.siam.org/journals/ojsa.php EXPLICIT VARIATIONAL FORMS FOR THE INVERSES OF Copyright © by SIAM . Unauthorized reproduction of this articl. , *44*(4), 2666–2694.

McLean, W. (2000). *Strongly elliptic systems and boundary integral equations*. Cambridge University Press, Cambridge.

Niu, J., Luo, M., & Liu, Q. H. (2014, July). Boundary integral spectral element method for extreme ultraviolet multilayer defects analyses. *2014 IEEE Antennas and Propagation Society International Symposium (APSURSI)*, 1994–1995. Retrieved from http://ieeexplore.ieee.org/lpdocs/epic03/wrapper.htm?arnumber=6905324 doi: 10.1109/APS.2014.6905324

Philbin, T. G. (2014). Making geometrical optics exact. *J. Modern Opt.*, *61*(7), 552–557. Retrieved from http://dx.doi.org/10.1080/09500340.2014.899646 doi: 10.1080/09500340.2014.899646

Rudin, W. (2006). *Real and complex analysis*. Retrieved from http://scholar.google.com/scholar?hl=en&btnG=Search&q=intitle:Real+and+complex+analysis#0 doi: 10.2307/2348852

Saad, Y. (2002). *Iterative methods for sparse linear systems* (Second ed.). Society for Industrial Mathematics.

Saad, Y. (2003). *Iterative Methods for Sparse Linear Systems: Second Edition*. Society for Industrial and Applied Mathematics. Retrieved from http://books.google.cl/books?id=ZdLeBlqYeF8C

Saad, Y., & Schultz, M. H. (1986, July). Gmres : A generalized minimal residual algorithm for solving non symetric linear systems. *SIAM J. Stat Comput.*, *vol. 7*(No. 3).

Sadiku, M. N. O. (1992). *Numerical Techniques in Electromagnetics*. Retrieved from http://www.crcnetbase.com/doi/book/10.1201/9781420058277 doi: 10.1201/9781420058277

Samuel P. Groth, S. L., David P. Hewett. (2013). *Hybrid numerical-asymptotic approximation for high frequency scattering by penetrable convex polygons* (Preprint No. MPS-2013-02). Department of Mathematics and Statistics, University of Reading.

Sauter, S., & Christoph, S. (2010). *Springer Series in Computational Mathematics, vol 39*.

Sommerfeld, A. (1949). *Partial differential equations in physics*. Elsevier Science. Retrieved from http://books.google.cl/books?id=PFsDVARE4C0C

Steinbach, O. (2008). Numerical Approximation Methods for Elliptic Boundary Value Problems. Retrieved from http://link.springer.com/10.1007/978-0-387-68805-3 doi: 10.1007/978-0-387-68805-3

Steinbach, O., & Wendland, W. (1998). The construction of some efficient preconditioners in the boundary element method. *Advances in Computational Mathematics*, *9*, 191–216. doi: 10.1023/A:1018937506719

Trefethen, L. N. (2013). *Approximation theory and approximation practice*. Society for Industrial and Applied Mathematics (SIAM), Philadelphia, PA.

Warnick, K. (2008). Numerical Analysis for Electromagnetic Integral Equations. *Artech House, Norwood, MA*.

Whitney, H. (2012). *Geometric Integration Theory*. Dover Publications. Retrieved from http://books.google.cl/books?id=d5vU2iVCcDMC

APPENDIX

APPENDIX 1. FURTHER SIMULATIONS

A. FURTHER SIMULATIONS

Until now, in all our simulation we have increased the permitivity and the number of modes. Is also of interest to see how the method works when the frequency increase. Figure 1.2(a) portrays errors for different exterior wavenumbers κ_0 and given contrasts using a fixed $N_i = 1.4k_i$ rule. This implies that for $\kappa_0 = 100$, the size of the linear system to solve is 1500×1500 ($\epsilon_{1,2} = 2$). If the same number of modes strategy is applied for the asymmetric case, the method fails to provide convergence. In this case, the strategy followed is to use the same maximum amount of modes achieving acceptable convergence errors. Figure 1.2(b), shows that even in the case of over-discretization the method is reliable. However, a robust rule of thumb is not clear. One can also observe an increase in error as frequency moves up. We are currently trying to determine whether this is inherent to our method or relate to the strategy used to set the number of modes.

Also we were able to compute the solution on other geometries. For example consider triangular geometry, as it can be see on figure 1.3(a). We fix the wave numbers asexterior wave number $\kappa_0 = 10$, interior wave numbers: upper left $\kappa_1 = 30$, upper right $\kappa_2 = 30$, lower left $\kappa_3 = 20$ and lower right $\kappa_4 = 20$, and increase the modes, as it can be see on figure (?, ?) the behaviour is totally different to the circular case. This can be easly explained because the singularities of the solution on the corners of the domain. Also, we compute the voulmen solution on figure 1.3(c), this was done with the repressentation formula 1.18.

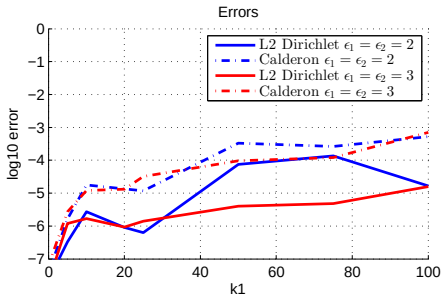

(a) Simetric case $N_i = 1.4k_i + 7$

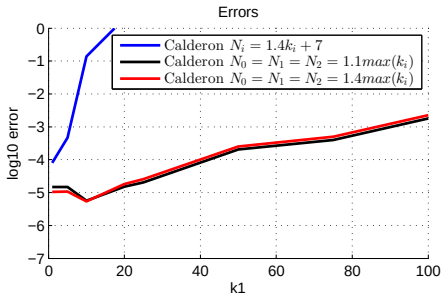

(b) Asimetric case $\epsilon_1 = 2, \epsilon_2 = 3$

Figure A.1. Frequency sweep results

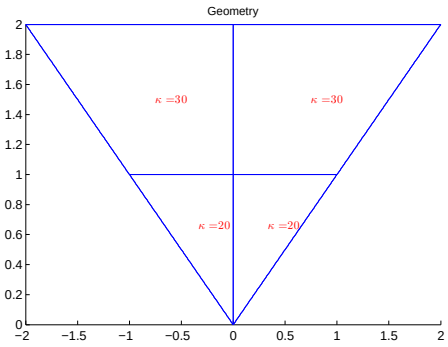

(a) Triangular geometry

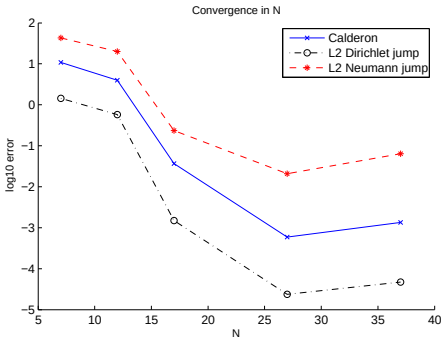

(b) Convergence on triangular geometry,

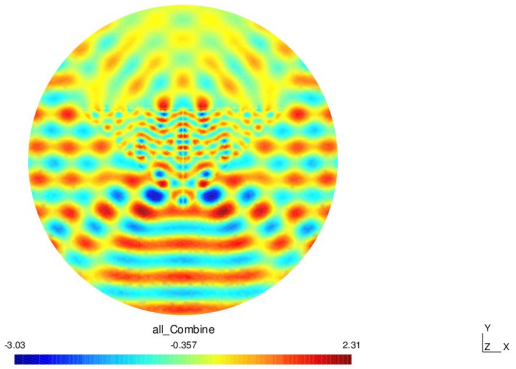

(c) Volumen solution, total field, on triangular geometry, incident angle $\alpha = \pi/2$.

Figure A.2. Triangular geometry